AgriEngineering

MDPI

Article

Spatio-Temporal Modeling of Land and Pasture Vulnerability in Dairy Basins in Northeastern Brazil

Jéssica Bruna Alves da Silva [1], Gledson Luiz Pontes de Almeida [1], Marcos Vinícius da Silva [2,*], José Francisco de Oliveira-Júnior [3,4], Héliton Pandorfi [1], Pedro Rogerio Giongo [5], Gleidiana Amélia Pontes de Almeida Macêdo [6], Cristiane Guiselini [1], Gabriel Thales Barboza Marinho [1], Ivonete Alves Bakke [2] and Maria Beatriz Ferreira [7]

1 Department of Agricultural Engineering, Federal Rural University of Pernambuco, Dom Manoel de Medeiros Avenue, SN, Dois Irmãos, Recife CEP 52171900, Pernambuco, Brazil; jessica.bruna@ufrpe.br (J.B.A.d.S.); gledson.almeida@ufrpe.br (G.L.P.d.A.); heliton.pandorfi@ufrpe.br (H.P.); cristiane.guiselini@ufrpe.br (C.G.); gabriel.bmarinho@ufrpe.br (G.T.B.M.)
2 Postgraduate Program in Forest Sciences, Federal University of Campina Grande, Santa Cecília, Patos CEP 58708110, Paraíba, Brazil; ivonete.alves@professor.ufcg.edu.br
3 Institute of Atmospheric Sciences, Federal University of Alagoas, Maceió CEP 57072260, Alagoas, Brazil; jose.junior@icat.ufal.br
4 Postgraduate Program in Architecture and Urbanism, Federal University of Alagoas, Maceió CEP 57072260, Alagoas, Brazil
5 Department of Agricultural Engineering, State University of Goiás, Via Protestato Joaquim Bueno, 945, Perímetro Urbano, Santa Helena de Goiás CEP 75920000, Goiás, Brazil; pedro.giongo@ueg.br
6 Department of Zootecnia, Federal Rural University of Pernambuco, Recife CEP 52171900, Pernambuco, Brazil; ameliazootecnia@gmail.com
7 Department of Forest Science, Federal Rural University of Pernambuco (UFRPE), Recife CEP 52171900, Pernambuco, Brazil; beatriz.ferreira2@ufrpe.br
* Correspondence: marcos.viniciussilva@ufrpe.br

check for updates

Citation: Silva, J.B.A.d.; de Almeida, G.L.P.; da Silva, M.V.; de Oliveira-Júnior, J.F.; Pandorfi, H.; Giongo, P.R.; de Almeida Macêdo, G.A.P.; Guiselini, C.; Marinho, G.T.B.; Bakke, I.A.; et al. Spatio-Temporal Modeling of Land and Pasture Vulnerability in Dairy Basins in Northeastern Brazil. *AgriEngineering* **2024**, *6*, 2970–3000. https://doi.org/10.3390/agriengineering6030171

Academic Editors: Jiang Chen, Lorena Nunes Lacerda and Lirong Xiang

Received: 27 June 2024
Revised: 5 August 2024
Accepted: 13 August 2024
Published: 20 August 2024

Abstract: The objective of this study is to evaluate the spatio-temporal dynamics of land vulnerability and pasture areas in the dairy basins of the states of Pernambuco and Alagoas, which are part of the Ipanema River Watershed (IRW) in the Northeast Region of Brazil. Maps of the Land Use and Land Cover (LULC); the Index of Vulnerability to Degradation (IVD); the Land Vulnerability Index (LVI); time series of Effective Herd (EH), Milked Cows (MC), and Milk Production (MP); and Pasture Cover (PC) and Quality (PCQ) were created as parameters. An opposite pattern was observed between the land use classes of Livestock, Agriculture, and Forest. The IRW area has predominantly flat terrain with a very high risk of degradation. The analysis of MC was consistent with the information from the EH analysis as well as with MP. When assessing Pasture Quality, Severe Degradation areas increased from 2010 to 2014, decreased after 2015, and rose again in 2020. Moderate Degradation areas remained high, while Not Degraded pasture areas were consistently the lowest from 2012 to 2020. Over the 10 years analyzed (2010–2020), the area showed a strong degradation process, with the loss of approximately 16% of the native vegetation of the Caatinga Biome and an increase in pasture areas and land vulnerability.

Keywords: caatinga; land vulnerability; cattle farming; semiarid; pasture quality

1. Introduction

Climate change and its impacts are among the most challenging threats the world faces today [1]; according to the future climate projections of this report, the expected increase in the duration and intensity of extreme heat waves and changes in the distribution of precipitation, water availability, and drought could reduce agricultural productivity and increase the risk of food insecurity.

The long-term trend of climate change and global warming is particularly pronounced in semiarid regions [2]. These regions are characterized by low rainfall and high temperatures, and already face significant challenges in ensuring food security and economic development [3]; in addition, climate change is causing even more water scarcity and increasing the frequency and intensity of extreme weather events, such as droughts and heat waves [4,5].

According to Andrade et al. [6] and Maranhão et al. [7], semiarid regions account for approximately 40% of the Earth's surface and around 50% of the population living in these regions obtain their basic needs (water, food, fiber, energy, etc.) from the goods and services generated in these ecosystems.

The Brazilian semiarid region occupies all the states of the Northeast Region of Brazil (NEB), with an area of 1,006,738 km^2, covering the territorial limits of 1171 municipalities with an estimated population of 26,378,043 inhabitants [8,9]. These regions are under the domain of the Caatinga Biome, an exclusively Brazilian biome with an extension of 982,563 km^2, occupying the equivalent of 11% of the entire national territory, which suffers from a high variability of rainfall, with little spatial distribution and concentrated over time [9]. In this sense, it has a highly dynamic vegetation cover, which requires constant monitoring of the changing conditions of the different land uses [5,10]. It is estimated that the net continuous loss of vegetation cover is in the order of 0.3% per year [11]. In addition, native areas still share space with agricultural crops, pastures, and herbaceous landscapes that alternate with bare soil [12].

In the semiarid region, subsistence farming is the primary economic activity and forms the foundation of rural society in most of the small municipalities there [13]. Medeiros et al. [14] and Vieira et al. [10] note that rainfed agriculture is the dominant agricultural system in this area. Typically practiced on small properties, this system involves growing subsistence crops through the burning of native vegetation and conventional soil preparation, alongside extensive livestock farming.

Agricultural and livestock production can result in the degradation of ecosystems, contamination of food, soil, and water, an increase in the cost of water collection for human supply, and an increase in greenhouse gas emissions through deforestation [15]. This scenario leads the scientific community to adopt more integrative approaches to address the problem, considering both climate change and sustainable development, with special attention given to arid and semiarid areas; these areas typically have low fertility and sparse vegetation cover, characteristic of fragile ecosystems, with a greater aptitude for desertification, marked by adverse climatic conditions and social vulnerability. Desertification is a global problem, affecting about a third of the planet's land surface, especially in arid and semiarid regions, and is characterized by soil erosion, reduced water quality, and the loss of biodiversity, damaging agriculture, livestock, and the livelihoods of local populations [16].

Given this scenario, it can be asserted that the sustainability of livestock farming depends on multiple factors and there is no definition of sustainability that fits all production worldwide, nor is there a single agricultural system that is more sustainable than alternative systems [17,18]. In other words, the sustainability of production in some regions may change as climate change affects water availability and agricultural production [19,20].

Pastures are the most practical and economical way to feed cattle, guaranteeing low production costs. However, inadequate management and the use of high stocking rates, which exceed the pasture's carrying capacity [15], contribute to its degradation and the stigmatization of extensive livestock farming as an unproductive activity that is essentially harmful to the environment [21]. According to Silva et al. [22], pastureland is the main land use in Brazil, occupying approximately 20% of the country's land, and is the main source of food for commercial livestock farming. According to the latest census by the Brazilian Institute of Geography and Statistics (IBGE), 47% of production units in the agricultural sector are made up of pastures, either natural and/or planted [23], and their degradation is

an aggravating factor in the Brazilian agricultural scenario, directly impacting meat and milk production. [24].

Pastures in the semiarid NEB face serious forage production problems due to the scarcity of rainfall [25]. Considering that they are mainly composed of native pasture of the region [26], this confirms that degraded pastures can reduce resources, indicating land abandonment; capital flight; or the temporary suspension of activities, including dairy farming, resulting in decreased economic activity in the affected areas [27].

Similar concerns can be observed in other studies, such as the work of Muralikrishnan et al. [28], who evaluated the impacts of climate change-induced drought on semi-arid pastoral and agricultural watersheds in South Asia, revealing reductions in surface and groundwater availability, soil degradation, partial or total crop loss, increased agricultural fallows and devastated lands, loss of biodiversity, and decreased agricultural production, pastures, and livestock in drought-impacted South Asia. Weng et al. [29] conducted a vulnerability assessment of a semiarid pastoral socio-ecological system in China, highlighting that livestock farming is central to the economic sector in semiarid regions, which rely on natural or seeded pastures for livestock feed, making them more vulnerable to climate change. Ndiritu [30] also conducted a study in Laikipia County, Kenya, evaluating the role of perceived climate extremes and access to private pastures on farms. Fust and Schlecht [31] analyzed the vulnerability of semiarid pasture systems to increased variability in the temporal distribution of precipitation events in the face of climate change. Nandintsetseg et al. [32] studied the risk and vulnerability of Mongolia's pastures under climate change, concluding that mitigating the adverse impacts of climate change on ecosystems, livestock, and pastures through strengthened coping capacities, risk reduction strategies, and resilience in degraded environments is a crucial challenge.

Furthermore, it is estimated that 75% of the earth's surface is under some degree of soil degradation, and this is expected to increase to 90% by 2050 [33]; however, according to the authors, estimates of land degradation are not conclusive and show large discrepancies. Inconsistencies between studies are attributed to the methods applied, which capture different aspects of degradation but neglect the whole picture; the most commonly used methods are expert opinion, satellite images, biophysical models, and abandoned farmland [34]. Of all the methods, perhaps the most accurate is that based on satellite images, as they show the actual degradation of the soil and are not limited to certain types of land use [35].

In this context, this study aimed to evaluate the spatio-temporal dynamics of land vulnerability and pasture areas in the dairy basins of the states of Pernambuco and Alagoas, inserted in the Ipanema River Watershed, in the Northeast Region of Brazil.

2. Materials and Methods

2.1. Study Area

The Ipanema River Watershed (IRW) is situated in the Caatinga Biome and has a semiarid climate; it covers two of the primary dairy basins in the states of Pernambuco and Alagoas, with an expanding area dynamic [9,13] between parallels 08°18′04″ S–10°0′ S and meridians 36°0′ W and 38°0′ W (Figure 1), with altitudes of less than 1115 m [36]. According to the Köppen-Geiger climate classification, the region predominantly experiences a BSh and As climate, characterized by a hot semiarid climate [37,38] with maximum temperatures occurring in the months from November to January (33 °C), minimum temperatures occurring in the months from May to July (19 °C), and average annual temperatures above 23 °C; the rainy season is more concentrated between the months of March and July, with an annual average of less than 700 mm [39,40]. The average annual potential evapotranspiration is also high, with rates that can exceed 1600 mm [40].

World milk production grew by 1.3% in 2019, according to FAO [41]. It is projected that global milk production will grow by 1.6% annually during the forecast period until 2029, growing faster than most other major agricultural products. The main producers, in order, are India, the European Union, the United States, Pakistan, China, Brazil, Russia, Turkey, New Zealand, and the United Kingdom.

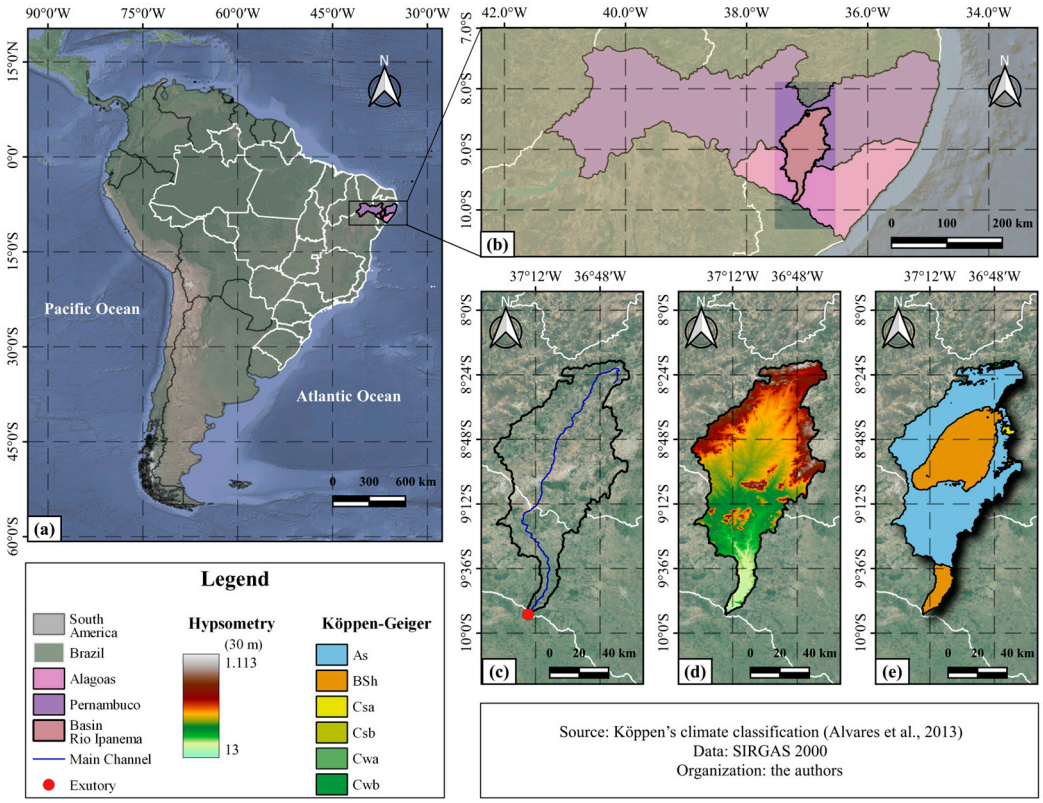

Figure 1. Location of the study area [37]. (**a**) Continental and national delimitation; (**b**) state delimitation and Ipanema River Basin; (**c**) delimitation of the main bed of the Ipanema River and identification of its mouth; (**d**) hypsometry based on the shuttle radar topography mission (SRTM) digital elevation model (DEM), with a spatial resolution of 30 m; (**e**) Köppen-Geiger climate classification of the Ipanema River Basin (IRW), Pernambuco and Alagoas, Brazil.

In Brazil, milk production is present in 99% of Brazilian municipalities, being one of the most traditional and important activities for the country's food security. Despite all the difficulties, Brazilian milk production grew by 139% between 1990 and 2019 [42].

According to Embrapa [43], milk production was estimated at 35.3 billion liters in 2021. Among the regions, only the Northeast, ranked third, experienced a growth in production (12.8%) and reached the mark of 5.5 billion liters, with the states of Pernambuco and Alagoas occupying seventh and 11th place, respectively, in the national ranking.

The dairy basins of Pernambuco and Alagoas are part of the IRW, with an area of approximately 7850 km^2, predominantly situated in the state of Pernambuco with its southern part extending into the state of Alagoas (Figure 2) and positioned within two significant hydrographic levels: the large São Francisco River Basin (macro-region) and the Lower São Francisco River Basin (meso-region) [44]. The term "dairy basin," although a local Brazilian concept, aligns with what is known as a "Milk Production Region/Zone" in the European Union or "Dairy Belt" in the United States, descriptions of geographic areas where milk production is high or where dairy farming is a dominant agricultural activity [45,46].

Data from the 2017 Agricultural Census [23] show that Alagoas had an effective herd of 786,018 animals (17.6%—Ipanema River Basin), of which 81,599 were dairy cows (41.8%—IRW), which generated the production of 188,628 (×1000) kg of milk (51.3%—IRW), distributed in 16 municipalities. Pernambuco, on the other hand, had 1,284,796 heads (22.5%—IRW), of which 222,344 were dairy cows (40.8%—IRW), which produced 520,990 (×1000) kg of milk (56.1%—IRW), distributed across 18 municipalities in Pernambuco, according to Table 1.

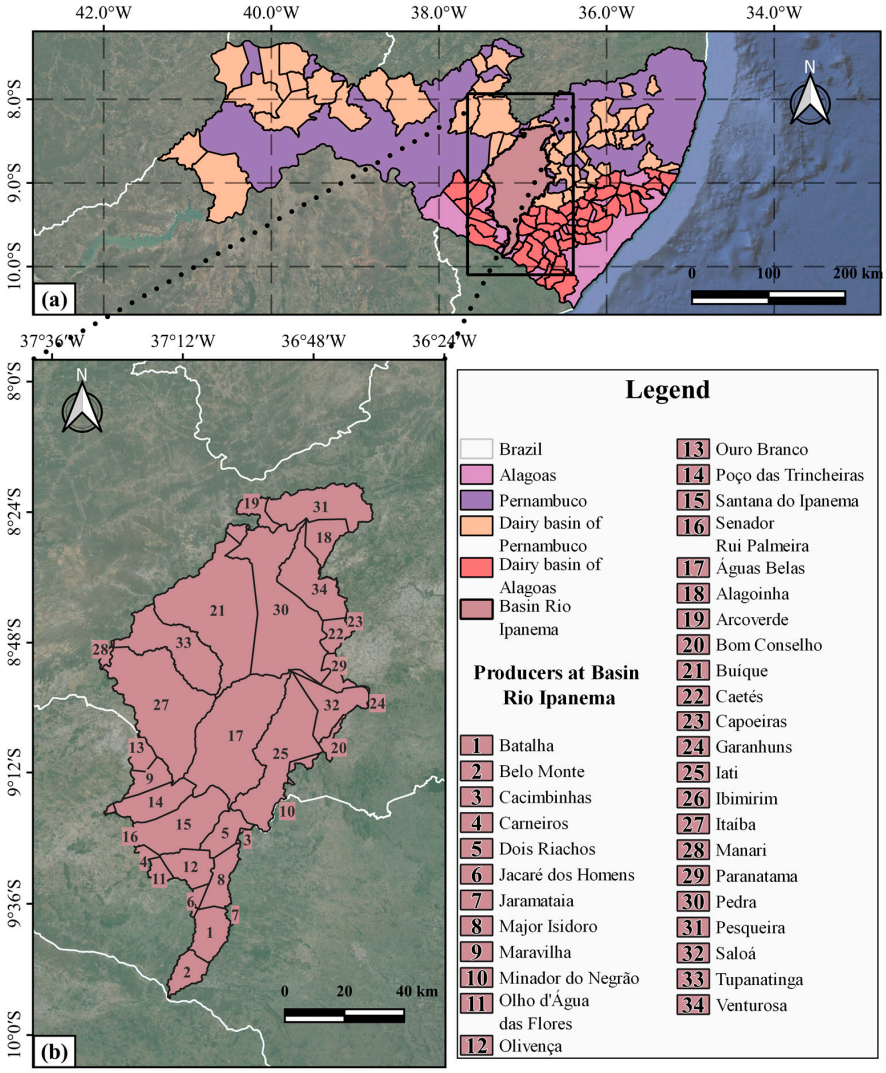

Figure 2. Municipalities within the dairy basins of Alagoas and Pernambuco that are part of the Ipanema River Basin (IRW). (**a**) State delimitation, Ipanema River Basin, and dairy basins of the states of Alagoas and Pernambuco, Brazil; (**b**) dairy-producing cities within the IRW.

Table 1. Comparison of dairy farming across states within the Ipanema River Basin and their respective percentages.

	State	
	Alagoas	**Pernambuco**
	Total (2017)	
Bovines (unit)	786,018	1,284,796
Cows Milked (unit)	81,599	222,344
Milk Produced (×1000)	188,628	520,990
	Basin Rio Ipanema	
Bovines (unit)	138,325	288,580
Cows Milked (unit)	34,129	90,785
Milk Produced (×1000)	96,778	292,533
	% Illustrative (Basin/Total)	
Bovines (unit)	17.6	22.5
Cows Milked (unit)	41.8	40.8
Milk Produced (×1000)	51.3	56.1

Source: Adapted from Agro Census 2017 [23].

2.2. Dynamics of Vegetation Cover via MapBiomas Brasil

The use of MapBiomas for studies on Land Use and Land Cover dynamics provides a robust, reliable, and high-quality database that is essential for understanding environmental changes and making informed decisions regarding sustainable land use. This is because it offers land cover data for the entire Brazilian territory with an extensive time series, allowing detailed analyses of changes over the years. Additionally, its standardized and recognized methodology ensures data consistency and comparability over time [47].

To evaluate vegetation cover, data for the study area were obtained from the MapBiomas platform [36]. Land use and Land Cover data can be accessed at: https://plataforma.brasil.mapbiomas.org/ (accessed on 20 October 2022).

MapBiomas operates with data collections and is currently at version 8.0. Each new collection involves reprocessing the entire historical dataset using updated methods and algorithms [36]. For this study, data from the most recent collection of version 6.0 were utilized; the collection includes a catalog of 25 legend classes from the platform, with a focus on the primary Level 1 classes: Forest (arboreal caatinga), Non-Forest Natural Formation (shrubby caatinga), Agriculture and Livestock, Non-Vegetated area (Urban Infrastructure and Exposed Soil), and Water bodies.

Raster files for the years 2010 to 2020 were generated for each land use type, and the predominant classes were computed using the "r.report" plugin in GRASS 7 software, integrated with QGIS 3.22.

2.3. Orbital Satellite Data: Landsat 5—Thematic Mapper (TM) and Landsat 8—Operational Land Imager (OLI)

The integration of geoprocessing with remote sensing techniques and satellite data are alternatives for monitoring land vulnerability, making it essential and economically viable for analyzing the spatio-temporal dynamics of Land Cover and Land Use changes [48,49], so that conservation management techniques can be established (agroforestry systems with animals, agroecological management of pastures, conservation agriculture, and crop–livestock–forestry integration), providing less pessimistic future scenarios and supporting decision making and planning for the sustainable use of agricultural activity.

Landsat satellites play a crucial role in monitoring the Earth's surface, with a spatial resolution of 30 m, which is sufficiently detailed to identify and analyze vegetation patterns and land use on regional scales. They also offer an extensive time series dating back to 1972, allowing for long-term analysis of changes in Land Cover and Land Use, and are widely available and accessible to the public, often at no cost [50,51].

The Normalized Difference Vegetation Index (NDVI) is a widely used index for monitoring vegetation, classifying land use, analyzing environmental changes, and managing natural resources. Thus, the combination of Landsat data and NDVI calculation provides a powerful tool for monitoring, analyzing, and managing Land Use and Land Cover, contributing to a better understanding of environmental dynamics and informed decision-making [51–53].

This study utilized orbital images from the Landsat-5 satellites with the TM sensor and the Landsat-8 satellite with the OLI sensor (Table 2), specifically, from orbit/point 215/066, provided by the United States Geological Survey (USGS) through the National Aeronautics and Space Administration (NASA). On average, 10 orbital images were processed annually from 2010 to 2020. It is important to note that indices for 2012 could not be generated due to a lack of coverage from the Landsat series for that period.

Table 2. Features of the multispectral bands from the Landsat 5 (TM) and Landsat 8 (OLI) satellites.

	Band	Spectral Resolution (μm)	Spatial Resolution (m)	Temporal Resolution
TM sensor	r1: Blue	0.45–0.52	30	16 days
	r2: Green	0.52–0.60	30	
	r3: Red	0.63–0.69	30	
	r4: Near Infrared	0.76–0.90	30	
TM sensor	r5: Near Infrared	1.55–1.75	30	
	r6: Thermal	10.40–12.50	120	
	r7: Mid Infrared	2.08–2.35	30	
OLI sensor	r1: Costal Aerosol	0.43–0.45	30	16 days
	r2: Blue	0.45–0.51	30	
	r3: Green	0.53–0.59	30	
	r4: Red	0.64–0.67	30	
	r5: Near Infrared	0.85–0.88	30	
	r6: SWIR 1	1.57–1.65	30	
	r7: SWIR 2	2.11–2.29	30	
	r8: Panchromatic	0.50–0.68	15	
	r9: Cirrus	1.36–1.38	30	
	r10: Thermal Infrared 1	10.6–11.19	100	
	r11: Thermal Infrared 2	11.50–12.51	100	

Source: Adapted from USGS/NASA [54].

To develop thematic maps of land vulnerability, based on geospatial and biophysical parameters, the NDVI was determined, developed, managed, and processed automatically using the Google Earth Engine (GEE) digital cloud platform (https://earthengine.google.com/ accessed on 10 October 2022) with JavaScript programming. This platform offers libraries equipped with a range of functions for mathematical analysis, modeling, statistical analysis, and machine learning, utilizing specific algorithms for the digital processing of satellite images [55].

The images used were sourced from the ee.ImageCollection ("LANDSAT/LT05/C02/T1_L2") and ("LANDSAT/LC08/C02/T1_SR") collections, covering surface reflectance products from 1 January 2010 to 31 December 2020. The dry period was defined as September, October, November, December, and January, while the rainy period included March, April, May, June, and July each year. A cloud cover threshold of less than 20% was applied, and the average image for each period was computed based on this criterion. However, for 2011, the minimum cloud cover criteria were adjusted to 30% for the dry period and 55% for the rainy period due to the lowest available cloud percentages for image acquisition. Thematic maps were classified and generated using QGIS 3.22.

2.4. Determining and Classifying Land Slope

The study of the risk of soil degradation is essential for maintaining agricultural productivity, preserving ecosystems, mitigating climate change, supporting economic sustainability, managing natural resources, and ensuring human well-being [56].

That said, the slope map was generated using a mosaic of digital images of altimetry data from the SRTM/NASA project, from quadrants s10_w038, s10_w037, s09_w038, and s09_w037, essential for understanding the region's topography and its impact on vulnerability to soil degradation. Using the "Raster Analysis—Reclassify by Table" processing tool, available in QGIS 3.22, the classification was carried out according to the limits of the slope classes referring to the risk of land degradation in order to obtain the Index of Vulnerability to Degradation (IVD) shown in Table 3.

Table 3. Slope classes related to the risk of land degradation.

Degradation Risk Class	Class Limits
Very Low	0 to 3
Low	3 to 6
Average	6 to 12
High	12 to 20
Very High	>20

Source: Lopes and Campos [57].

The relief slope classification (Table 4) was carried out according to the methodology proposed by Embrapa [58].

Table 4. Slope classes according to methodology proposed by EMBRAPA [58].

Slope Class	Class Limits (%)
Flat	0–3
Soft Wavy	3–8
Wavy	8–20
Strong Wavy	20–45
Hilly	45–75
Cliff	>75

2.5. Land Vulnerability Index (LVI)

The LVI was calculated by processing the images in QGIS 3.22, as shown in Figure 3.

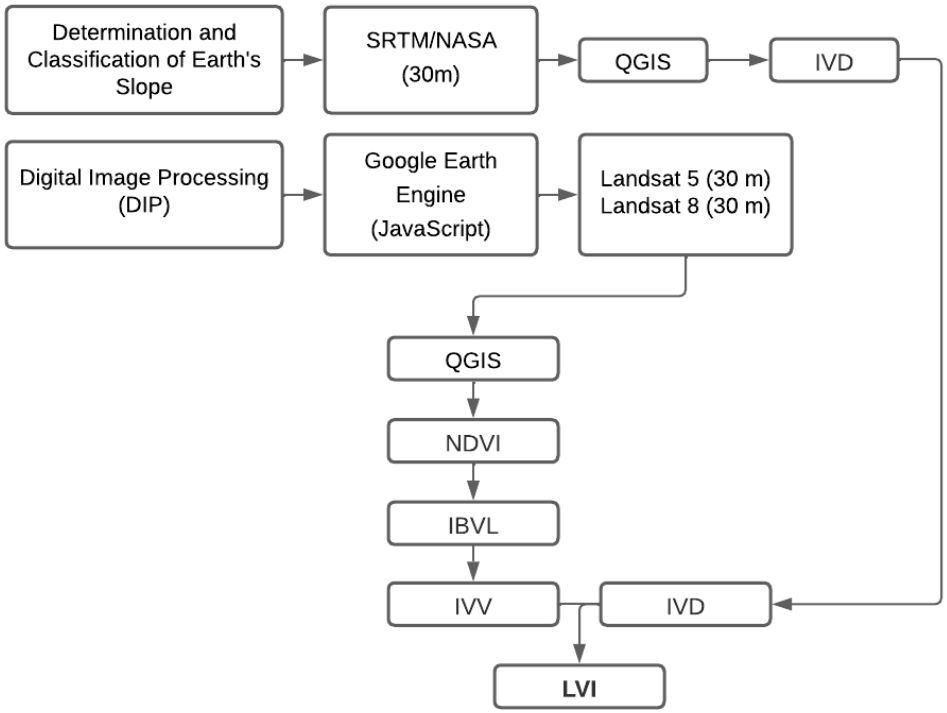

Figure 3. Image processing flowchart for calculating the Land Vulnerability Index (LVI). Note: SRTM = Shuttle Radar Topography Mission; NASA = National Aeronautics and Space Administration; QGIS = Quantum Geographic Information System; IVD = Index of Vulnerability to Degradation; NDVI = Normalized Difference Vegetation Index; IBVL = Woody Vegetation Biomass Index; IVV = Vegetation Vulnerability Index; LVI = Land Vulnerability Index.

NDVI is a sensitive measure of vegetation health, with values ranging from −1 to 1. Values close to 1 indicate high levels of photosynthetically active vegetation, while

values near zero suggest minimal or no vegetation. Negative values typically denote water bodies [49]. NDVI was determined according to Equation (1) [59,60].

$$\text{NDVI} = \frac{r_{b\ \text{NIR}} - r_{b\ \text{RED}}}{r_{b\ \text{NIR}} + r_{b\ \text{RED}}} \quad (1)$$

where rb NIR and rb RED correspond to the respective reflective bands 4 and 3 of the Landsat-5 TM sensor and 5 and 4 of the Landsat-8 OLI sensor.

The NDVI was employed to reclassify vegetation (Table 5), using the Woody Vegetation Biomass Index (IBVL) method proposed by Chaves et al. [61], to assess and describe vegetation in the Caatinga at various stages of anthropization.

Table 5. Vegetation and slope classes and indices for estimating land vulnerability.

Vegetation Classes	Vegetation		Slope	Vulnerability	
	IBVL *	IVV	IVD	LVI	Class
Very Dense Tree Dense Tree	1.00 0.80	1.00 1.25	0 a 3	0 a 6	Very Low
Dense Undergrowth Dense Shrubby Undergrowth	0.68 0.60	1.47 1.67	3 a 6	6 a 12	Low
Dense Sub-Tree Shrub Open Sub-Tree Shrub	0.48 0.36	2.08 2.78	6 a 12	12 a 24	Moderate
Open Sub-Shrub Shrub Thin Shrubby Sub-Shrub	0.24 0.14	4.17 7.14	12 a 20	24 a 40	High
Very Sparse Shrubby Shrub Exposed Soil	0.07 0.05	14.29 20.00	>20	>40	Very High

* IBVL, Woody Vegetation Biomass Index; IVV, Vegetation Vulnerability Index; IVD, Index of Vulnerability to Degradation; LVI, Land Vulnerability Index.

The Vegetation Vulnerability Index (IVV), also developed by Chaves et al. [61], was estimated by calculating the difference between the IBVL for a hypothetical scenario of maximum preservation and the actual condition of the vegetation being evaluated, according to Equation (2).

$$\text{IVV} = \left(\frac{1}{\text{IBVL}}\right) \quad (2)$$

where "1" is the Woody Vegetation Biomass Index (IBVL) value for the condition of maximum preservation, while IBVL represents the Woody Vegetation Biomass Index for the evaluated vegetation condition.

The Land Vulnerability Index (LVI) was calculated as the product of the Vegetation Vulnerability Index (IVV) and the Index of Vulnerability to Degradation (IVD), following Equation (3).

$$\text{LVI} = \text{IVV} \times \text{IVD} \quad (3)$$

To map the vulnerability of the basin's land, data on the vegetation and slope parameters were cross-referenced, as shown in Table 5.

2.6. Characterization of the Cattle Herd, Milked Cows and Milk Production Time Series by Municipality

Quantifying the herd and its production and productivity is essential for understanding and mitigating the impacts of livestock on soil degradation, promoting sustainable land use, and ensuring environmental conservation and economic and social sustainability [62].

In this way, a survey was carried out to quantify the Effective Herd (EH), Milked Cows (MC), and Milk Production (MP) in each of the 34 municipalities studied in the 2010–2020 period using the Municipal Livestock Survey (PPM) database from the Automatic Recovery System (SIDRA) platform of the Brazilian Institute of Geography and Statistics (IBGE) via

the following email address: https://sidra.ibge.gov.br/pesquisa/ppm/quadros/brasil/2021 (accessed on 20 October 2022).

Thematic maps were created to visualize the temporal spatialization of the EH, MC, and MP of the municipalities in the dairy basin included in the IRW in the years 2010 and 2020, by making shapefile (.shp) and raster files, combining the data obtained from SIDRA and the geographical data from IBGE, using QGIS 3.22.

2.7. Pasture Cover Dynamics via the Pasture Atlas

The study of pasture cover dynamics is essential for optimizing livestock production, ensuring environmental sustainability, improving resource efficiency, and adapting to climate change, contributing to a more productive and sustainable dairy farming system [63,64].

Pasture data for the study region were extracted from the Pasture Atlas platform of the Image Processing and Geoprocessing Laboratory of the Federal University of Goiás (PAPIG/UFG). The data are available at: https://atlasdaspastagens.ufg.br/map (accessed on 20 October 2022).

The pasture mapping used in the platform is based on images from the Landsat satellite series; the Random Forest supervised classifier and robust statistical sampling techniques (for calibration and validation of the classification models) were used, with an overall accuracy of approximately 91% [65].

The shapefile files were generated and transformed into raster files for the years 2010–2020 and processed using QGIS 3.22.

2.8. Pasture Quality via MapBiomas Pasture

The Pasture Quality data were extracted from the MapBiomas Brasil platform, from Collection 6, which is available at: https://plataforma.brasil.mapbiomas.org/ (accessed on 20 October 2022).

According to MapBiomas [66], Brazil's main land use is pasture, which occupies an area of 154 million hectares, from the north to the south of Brazil, and is present in all of Brazil's Biomes. The Caatinga Biome, in 2020, had a total pasture area of around 20.2 million hectares; in percentage terms, it is the third most occupied Biome by cultivated pastures, of around 23.1%, with the most occupied being the Atlantic Forest (25.7%) and the Cerrado (23.7%).

The raster files were processed in QGIS 3.22 and the thematic maps were produced and classified into three main classes: severely degraded, moderately degraded, and not degraded.

2.9. Statistical Procedures

Principal component analysis (PCA) was carried out using the variables LVI, MapBiomas classes (5 classes), number of livestock, and pasture in the dry and rainy periods, for the series from 2010 to 2020. Based on the principal components (PC), the covariance matrix was obtained to extract the eigenvalues that originate the eigenvectors. The Kaiser criterion was used to identify the variables that showed correlation, considering eigenvalues greater than 1.0, which generate components with a relevant amount of information contained in the original data [67,68].

Finally, Pearson's correlation (r) was carried out for all the variables, seeking to correlate with the PCA, in order to highlight the similarities between the variables. The program used for PCA and Pearson's correlation was RStudio, version 3.6.1 [69].

3. Results and Discussion

3.1. Land Use and Cover Classes via MapBiomas Brasil

Between 2013 and 2015, the Northeast Region showed an annual growth in the agricultural sector of approximately 3374 ha, followed by a reduction in the native forest of the Caatinga Biome [9,70], which is considered one of the most threatened by environmental degradation due to the predominance of the semiarid climate [10]. Figure 4 shows the Land

Use and Land Classes (LULC) and Figure 5 shows the quantification of the area in hectares (ha) for the period from 2010 to 2020. An inverse relationship was observed between the Forest and Agriculture and Livestock classes; forested areas (Caatinga) decreased over time, while agricultural areas increased.

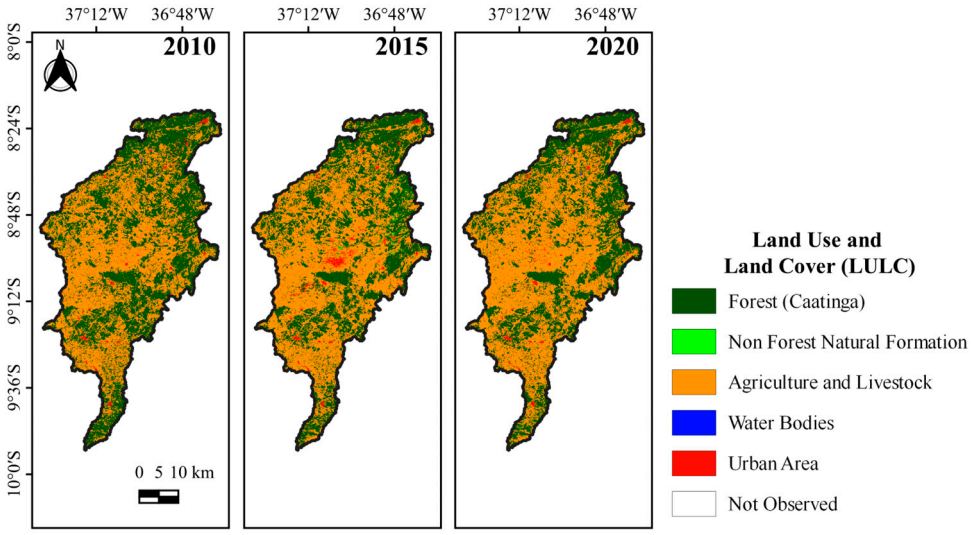

Figure 4. Change at 5-year intervals observed in spatio-temporal dynamics of LULC from 2010 to 2020 in the IRW.

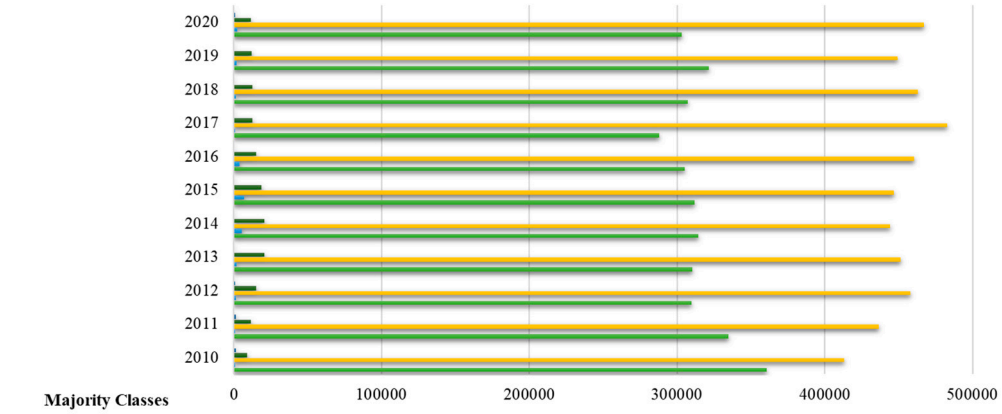

Majority Classes	2010	2011	2012	2013	2014	2015	2016	2017	2018	2019	2020
Not Observed	136	136	136	136	136	136	136	136	136	136	136
Water Bodies	1384	1265	769	414	277	218	230	459	545	507	847
Non Vegetated Area	8836	11,497	14,925	20,910	20,575	18,661	14,953	12,611	12,634	11,885	11,319
Agriculture and Livestock	413,033	436,723	458,080	451,157	444,012	446,850	460,547	483,126	463,212	449,270	467,227
Non Forest Natural Formation	994	781	1376	1928	5522	7171	4086	816	1115	1722	2395
Forest	360,616	334,597	309,714	310,454	314,478	311,963	305,048	287,852	307,358	321,480	303,077

Figure 5. Quantification of areas (ha) of Land Use and Land Cover for the years 2010–2020 in IRW.

In 2016 and 2017, the forest area was 305,047 ha and 287,852 ha, respectively. During the same years, the agricultural area increased from 460,547 ha to 483,125 ha, reflecting a reduction of 13,696 ha in forested land and an increase of 22,578 ha in agricultural and livestock areas (Figure 5). Additionally, the area of non-forest natural formations decreased by 3270 ha over this period, similar results can also be observed in the study by Fernandes et al. [71], who evaluated changes in Land Use and Land Cover (LULC) in the semiarid region of Sergipe between 1992 and 2017 using remote sensing data and techniques. They simulated changes in Land Use and Land Cover between 2017 and 2030 by applying a cellular automata model. The authors concluded that agricultural and livestock activities increased from 1992 to 2017, while forest areas decreased and were undergoing degradation

processes; these findings support the results reported by Silva et al. [68], who assessed land degradation in the semiarid region of the Ipojuca Valley. They also align with the work of Melo et al. [72], who analyzed Land Use and Land Cover changes in the Agreste region of Pernambuco, and Silva et al. [55], who investigated the environmental degradation of vegetation and water bodies in the semiarid region of the NEB.

Based on the observed data, it is important to highlight the overall accuracy of the MapBiomas classification for Collection 6 (Figure 6). For the study period and area, the accuracy ranged from a maximum of 84% to a minimum of 80%, with an average of 82.2% [73].

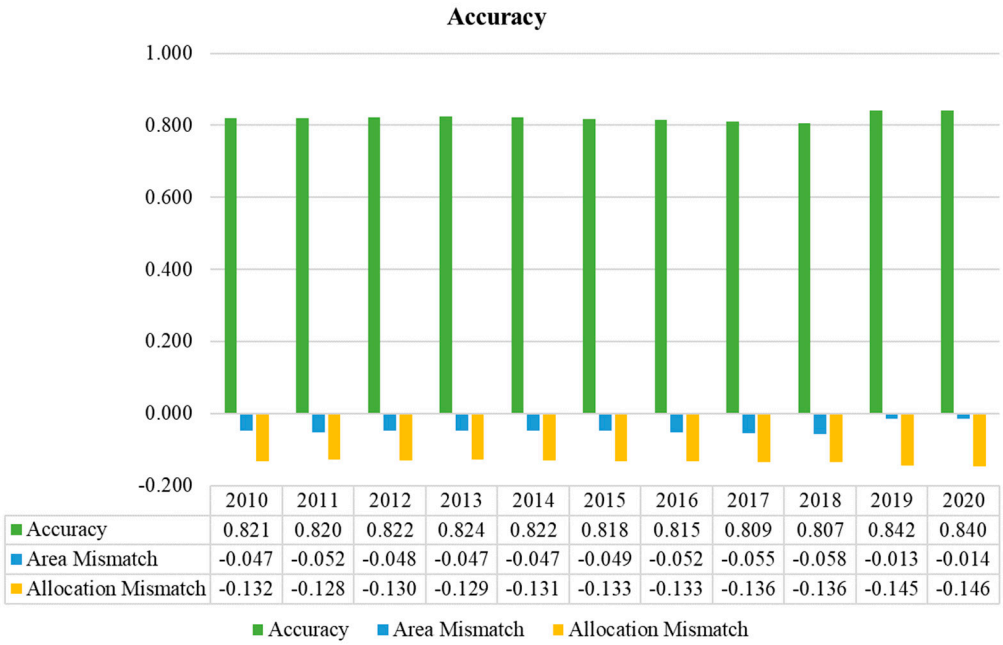

	2010	2011	2012	2013	2014	2015	2016	2017	2018	2019	2020
Accuracy	0.821	0.820	0.822	0.824	0.822	0.818	0.815	0.809	0.807	0.842	0.840
Area Mismatch	-0.047	-0.052	-0.048	-0.047	-0.047	-0.049	-0.052	-0.055	-0.058	-0.013	-0.014
Allocation Mismatch	-0.132	-0.128	-0.130	-0.129	-0.131	-0.133	-0.133	-0.136	-0.136	-0.145	-0.146

Figure 6. Accuracy of Level 1 MapBiomas Collection 6 for the years 2010–2020 across the dairy-producing municipalities in the IRW, located in the states of Alagoas and Pernambuco.

According to the Algorithm Theoretical Basis Document (ATBD), which outlines the process of map development and the algorithms used, the digital classification of Landsat mosaics in the Caatinga Biome combines the Agriculture and Pasture classes into a single category, making it impossible to distinguish between them. Additionally, the Unvegetated Areas category includes both Urban Areas and Exposed Soil. This could explain the potential discrepancies in the classification of the Agriculture and Livestock class for 2017, which recorded the largest area at 483,125 ha, significantly higher than other years that ranged from 460,000 to 463,000 ha (2016 and 2018, respectively). This occurred alongside the smallest Forest area (287,852 ha) of the entire series (2010–2020) and one of the smallest areas for the Non-Forest Natural Formation class (815.73 ha). It is important to note that this year also had the second-lowest value for the specified category's overall accuracy percentage (80.9%) [74] and the second-highest area mismatch (−0.055).

Another notable aspect is the data for the Non-Vegetated Area class (Urban Infrastructure and Exposed Soil). In 2012, this class covered 14,920 ha, which increased to 20,910 ha in 2013 and 20,574 ha in 2014, showing a rise of 5990 ha, before decreasing to 18,661 ha in 2015, a reduction of 335.40 ha. Given that features in this class are related, it is likely that the variation reflects changes in Exposed Soil areas. This pattern is evident in the region, where such changes typically occur after the harvest of crops used for grain production, silage forage, or grazing, until the rainy season returns and natural vegetation recovers, or a new crop is planted for the next cycle, corroborating the results of Bolfe et al. [25].

3.2. Analysis of Slope and Index of Vulnerability to Degradation (IVD)

The maps for determining the slope and the Index of Vulnerability to Degradation (IVD) show that the IRW area has predominantly flat terrain with a very high risk of degradation. Wavy and strongly wavy terrain corresponds to a low and very low risk of degradation (Figure 7).

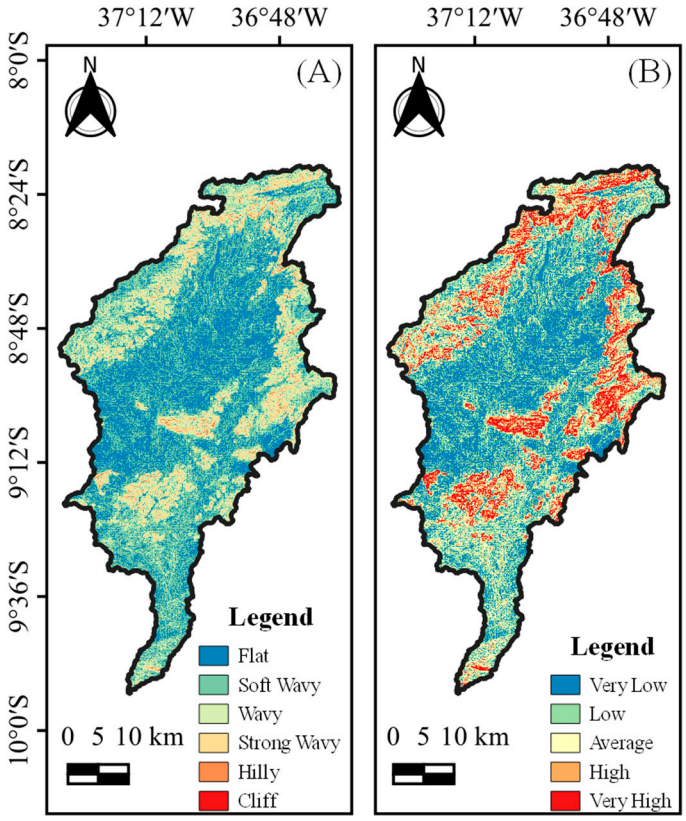

Figure 7. Classification of the slope according to the Embrapa Methodology (**A**) and the risk of degradation (**B**) of the area of the municipalities of the dairy basins of the states of Alagoas and Pernambuco, inserted in the IRW.

It was observed that the low and very low degradation risks are also directly related to the higher altitudes of the area (Figure 7B), where the slope effect is typically reduced by the higher levels of vegetation cover. This is associated with areas that are challenging to access, with shallow and sloping soils that are not suitable for agriculture [75], and are now destined for Legal Reserve Areas, in compliance with Law N°. 12,727, which sets forth general regulations for the protection of vegetation and Permanent Preservation Areas [76]. Furthermore, Tolche et al. [77], in their study of modeling and accessing land degradation vulnerability using remote sensing techniques, argue that slope was found to be the main factor determining land degradation.

Hossain et al. [78], who analyzed agricultural land degradation and processes that undermine future food security, indicated that, besides variations in land use practices and deforestation, the topography and slope of a landscape affects soil erosion and degradation, noting that even gentle slopes can lead to erosion due to their topographic positioning and exposure to anthropogenic actions.

Duguma and Janssens [79] proposed identifying the main constraints to livestock production in three highland regions within mixed crop–livestock production systems in southwestern Ethiopia. They concluded that pasturelands were degrading, with causes varying but primarily focusing on vegetation and soil erosion, underscoring the importance of evaluating the IVD (Index of Vegetation Degradation) in this study.

3.3. Evaluation Land Vulnerability Index (LVI)

The results obtained by the LVI corroborate the results obtained by the IVD, indicating that the IRW area has a high risk of land vulnerability and that the areas with the greatest vulnerability are those with flat and soft wavy terrain. For the dry period (Figure 8), the index remained high and constant throughout the series (2010–2020).

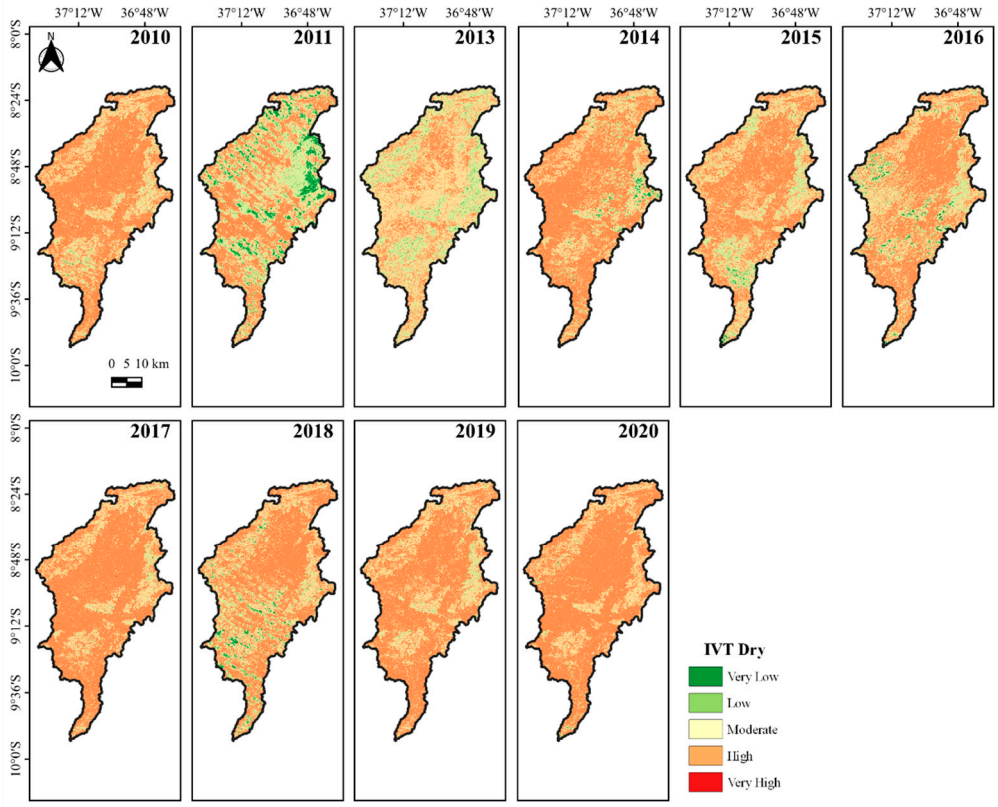

Figure 8. Spatio-temporal dynamics of the Land Vulnerability Index (LVI) for the dry season from 2010 to 2020 in IRW.

When comparing the land use and occupation maps via MapBiomas (Figure 4), it can be seen that the areas with a moderate LVI class are nearly always linked to low and very low vulnerability classes across the study area, corresponding to areas with forest (Caatinga). The areas at high and very high risk correspond to the Agriculture and Livestock classes. Similar results were found by Santos et al. [49] in their study on the causes and consequences of seasonal changes in the flow of the São Francisco River in the Brazilian semiarid region. The study revealed a predominance of high and very high classes, with average values of 15.3% and 58.5%, respectively, a situation exacerbated during drought periods due to the intrinsic characteristics of the Caatinga vegetation.

In the rainy season (Figure 9), the Vulnerability Index also remained high and constant throughout the series. The results were in agreement with the data from the dry season, where the areas with moderate, low, and very low LVI correspond to areas with Forest (Caatinga) and the areas with a high and very high risk correspond to areas in the Agriculture and Livestock classes, as they are easily managed, including, in some cases, the use of machinery, according to the land use and occupation maps (Figure 4). It can also be seen that in the rainy season, the decrease in the percentage of high and very high classes is attributed to the increase in rainfall distribution and volume, which leads to greater vegetation cover in this area, a result similar to that observed by Santos et al. [49].

Table 6 shows that, despite maintaining the high class, according to the Vulnerability Index, during the rainy season, there was a percentage reduction in the representation of this class in the area. This was also observed by Cantalice et al. [80] in a study of

laminar runoff in a semiarid environment, in which they found that the presence of native vegetation has a greater effect on protecting the soil cover, increasing rainfall interception and reducing surface runoff.

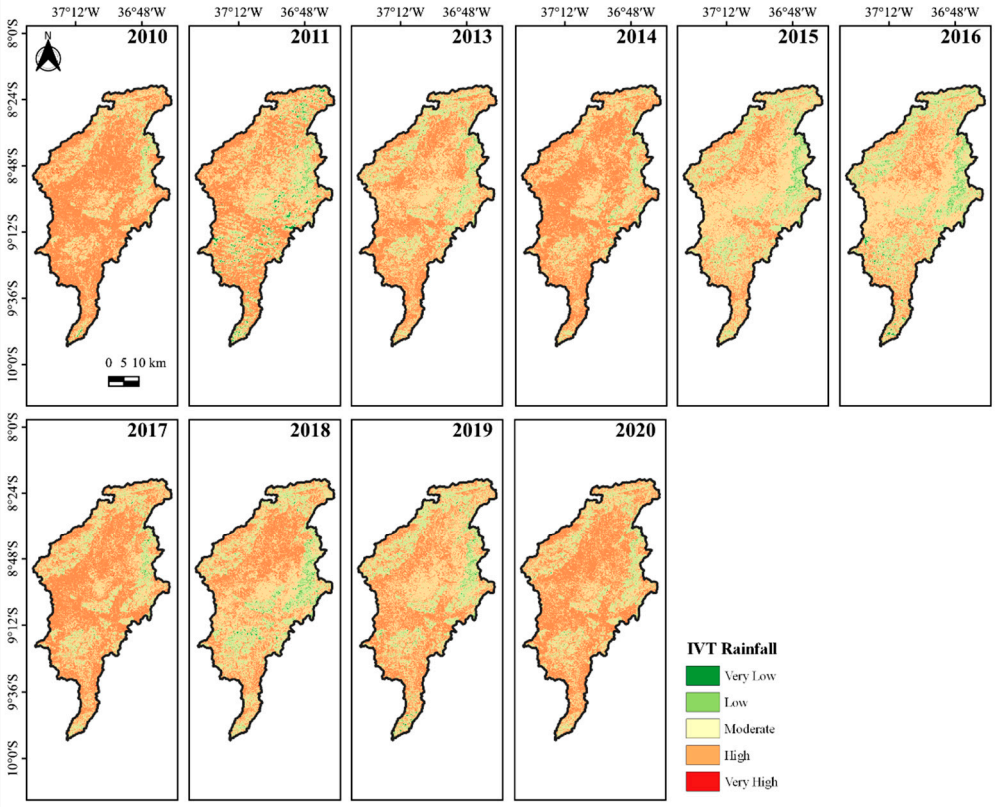

Figure 9. Spatio-temporal dynamics of the Land Vulnerability Index (LVI) for the rainy season from 2010 to 2020 in the IRW.

Table 6. Representative percentage of the areas of the Land Vulnerability Index (LVI) classes for the dry and rainy periods from 2010 to 2020 in the IRW.

LVI	Year	Class Area (%)				
		Very Low	Low	Moderate	High	Very High
Dry	2010	0.43	6.98	25.19	67.27	0.13
	2011	5.73	26.77	24.77	37.35	5.38
	2013	1.72	25.89	44.56	27.53	0.30
	2014	1.12	8.51	25.14	64.56	0.67
	2015	1.05	15.15	29.42	54.02	0.35
	2016	1.73	14.15	28.39	54.45	1.29
	2017	0.26	4.35	22.36	72.95	0.09
	2018	1.95	11.64	26.67	58.47	1.28
	2019	0.25	6.56	25.99	67.12	0.08
	2020	0.32	2.43	22.01	75.12	0.12
Rainy	2010	0.39	9.76	28.97	60.76	0.12
	2011	2.50	18.68	35.40	42.39	1.03
	2013	0.82	19.45	37.45	42.10	0.18
	2014	0.54	12.80	31.52	54.99	0.15
	2015	1.76	23.41	47.02	27.52	0.28
	2016	3.04	20.34	46.73	29.32	0.56
	2017	0.59	16.57	30.53	52.16	0.15
	2018	1.91	24.49	38.21	35.01	0.39
	2019	1.30	22.17	37.55	38.70	0.28
	2020	0.53	16.73	31.36	51.23	0.15

As noted above, the high vulnerability class was predominant in the area in almost all years, during the dry and rainy periods, with maximum values of 72.95% (2017) and 60.76% (2010), respectively. The moderate vulnerability class was the second most representative class, with values of 44.56% (2013) and 47.02% (2015) in the dry and rainy periods, respectively.

3.4. Time Series Analysis of the Herd, Milked Cows and Milk Production

The spatial analysis of the time series for EH (Animal Unit—AU) in the study area (Figure 10) showed that there was a drop in the number of AU between 2010 and 2012 in the municipality of Itaíba—PE (Figure 2), from 95,000 AU in 2010 to 100,000 AU in 2011 and 50,000 (AU) in 2012, a reduction of 50%. One possible reason for this drastic reduction in the number of AUs in the municipality was the attack by the carmine cochineal (Dactylopius opuntiae), which affected a large part of the region's palm groves, considered one of the main sources of forage for dairy cattle in the Northeast Region during the dry period of the year [81], causing extremely serious socio-economic consequences for all livestock activities, in addition to the hydrological years of below-average rainfall and severe droughts, especially between 2012 and 2016 [82,83]. Similar results were described by Montcho et al. [84], who reported dairy producers in West Africa perceiving an increase in the dry season and temperature, which led to a decrease in herd size, cattle fertility, milk production, forage availability, and milk preservation. From 2012 onwards, herd numbers in all municipalities remained stable, with little variation, with a maximum of 60,005 AU in Itaíba and a minimum of 3600 AU in Paranatama.

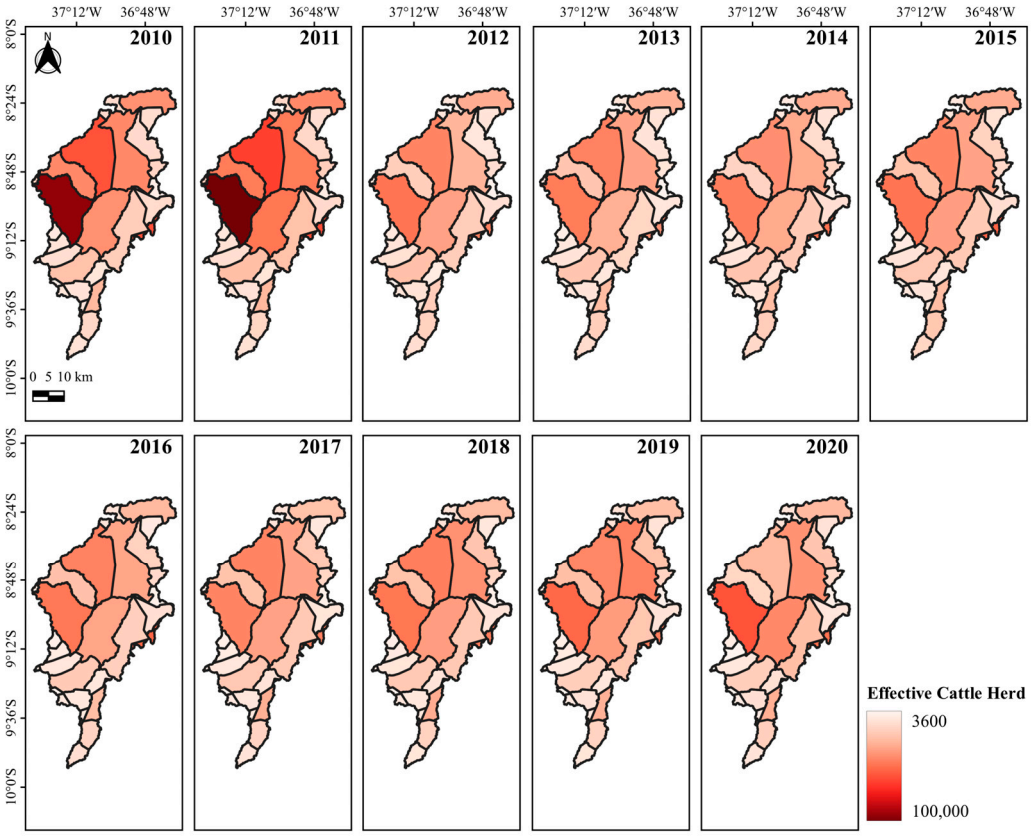

Figure 10. Spatio-temporal dynamics of the Effective Herd (EH) from 2010 to 2020 in the IRW.

According to the study by Seidou et al. [85], which evaluated the effect of integrated agricultural systems on daily milk production and demographic characteristics of dairy cows in drylands, monitoring the structure of a dairy herd provides important insights into herd profitability and farm dynamics, enabling the improvement of livestock integration practices adopted by farmers of this type.

The ranking of the municipalities representing the five largest EH can be seen in Table 7, where it is noted that there was little variation in positions. The municipality of Itaíba maintained the highest EH throughout the series, except during the period of 2014–2017, when the municipality of Bom Conselho occupied first place. There was also a fluctuation in the EH of the municipality of Buíque, which ranged between second and fourth place.

Table 7. Ranking of the five municipalities with the highest number of EH from 2010 to 2020 in IRW.

Year	Municipality				
	1°	2°	3°	4°	5°
2010	Itaíba	Bom Conselho	Buíque	Pedra	Tupanatinga
2011	Itaíba	Buíque	Bom Conselho	Águas Belas	Pedra
2012	Itaíba	Bom Conselho	Buíque	Águas Belas	Pesqueira
2013	Itaíba	Buíque	Bom Conselho	Pedra	Águas Belas
2014	Bom Conselho	Itaíba	Buíque	Pedra	Águas Belas
2015	Bom Conselho	Itaíba	Buíque	Águas Belas	Pedra
2016	Bom Conselho	Itaíba	Buíque	Águas Belas	Pedra
2017	Bom Conselho	Itaíba	Buíque	Águas Belas	Pedra
2018	Itaíba	Bom Conselho	Buíque	Pedra	Águas Belas
2019	Itaíba	Bom Conselho	Pedra	Buíque	Águas Belas
2020	Itaíba	Bom Conselho	Águas Belas	Pedra	Major Isidoro

Differences in management practices between regions and herd sizes can help define potential future approaches for research and extension. In this way, such studies can provide valuable information that will assist dairy producers in developing strategies for managing and administering their properties, aiming to improve production efficiency [86].

For the MC analysis (Figure 11), there was agreement with the information contained in the EH analysis, where the maximum value was 33,000 in the municipality of Itaíba (2011) and the minimum was 497 in Paranatama (2014). It can be seen that, as with the EH, the number of MC in the municipality of Itaíba fell between 2010 and 2012, from 30,000 to 18,000, respectively, a reduction of 45.5%, close to the 50% reduction in its EH; these reduction rates can be explained by the reduction in AU due to the attack by the carmine cochineal (*Dactylopius opuntiae*), which affected a large part of the region's palm groves, in addition to the hydrological years of below-average rainfall and severe droughts, highlighting the need for more effective and adaptive management strategies to address environmental challenges and maintain production sustainability.

The ranking of the five municipalities with the highest number of CM (Table 8) shows that although the municipality of Itaíba has had the highest EH for almost every year, the number of Milked Cows in the municipality was highest only during 2011–2012 and 2019–2020. The municipalities of Buíque, Pedra, and Bom Conselho are among the municipalities with the highest number of MC in the entire series.

The results demonstrate the importance of considering not only the production efficiency but also the stability and resilience of dairy systems. Although Itaíba led in EH for most of the analyzed period, its position in the ranking of the number of dairy cows varied, indicating that other municipalities, such as Buíque, Pedra, and Bom Conselho, have played significant roles in the milk production of the study area. These insights are crucial for formulating targeted policies and strategies that can enhance the efficiency and competitiveness of the dairy industry while promoting sustainable growth.

When analyzing MP (Figure 12), the pattern observed in the previous analyses was repeated. The MP of the municipality of Itaíba, during the first three years of the series, showed the same behavior, with an increase between the years 2010 and 2011 and a decrease in 2012, with values of 86,797 (×1000), 102,383 (×1000), and 59,625 (×1000), respectively, a reduction of 41.8% in production; this pattern highlights Itaíba's vulnerability to production fluctuations, which may be associated with environmental or management factors. As

expected, from the analysis of the previous variables, the municipality of Paranatama had the lowest MP, with 72 (×1000), following the pattern of the lowest EH and the lowest number of MC in 2014.

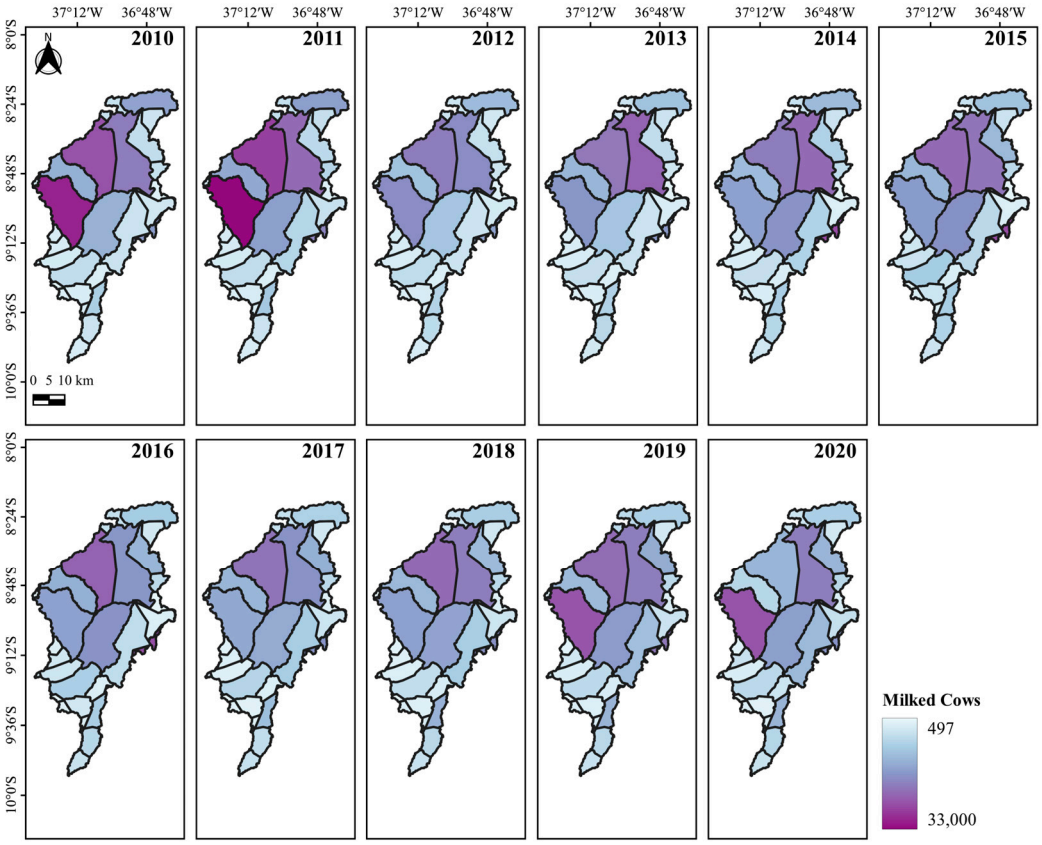

Figure 11. Spatio-temporal dynamics of milking cows (MC) from 2010 to 2020 in the IRW.

Table 8. Ranking of the five municipalities with the highest number of MC from 2010 to 2020 in IRW.

Year	Municipality				
	1°	2°	3°	4°	5°
2010	Itaíba	Buíque	Pedra	Bom Conselho	Pesqueira
2011	Itaíba	Buíque	Pedra	Bom Conselho	Pesqueira
2012	Buíque	Itaíba	Pedra	Bom Conselho	Pesqueira
2013	Pedra	Buíque	Itaíba	Bom Conselho	Tupanatinga
2014	Bom Conselho	Pedra	Buíque	Águas Belas	Itaíba
2015	Bom Conselho	Buíque	Pedra	Águas Belas	Itaíba
2016	Bom Conselho	Buíque	Águas Belas	Pedra	Itaíba
2017	Buíque	Pedra	Bom Conselho	Itaíba	Águas Belas
2018	Buíque	Pedra	Bom Conselho	Itaíba	Águas Belas
2019	Itaíba	Buíque	Bom Conselho	Pedra	Águas Belas
2020	Itaíba	Pedra	Bom Conselho	Águas Belas	Major Isidoro

The municipalities of Buíque, Pedra, and Bom Conselho continued to appear in the ranking (Table 9) among the municipalities with the highest MP in the series. Similar results were highlighted by Silva and Costa Júnior [87] in the study of ^{228}Ra in cow's milk from an anomalous region of Pernambuco, in which the municipality of Pedra is among the most relevant regarding milk production in the state of Pernambuco. According to IBGE [23], this region ranks as the second-largest milk-producing area in the NEB. Adding to this, the persistence of these municipalities in the ranking of the highest MPs throughout the series

highlights the importance of successful management and dairy production strategies in these areas.

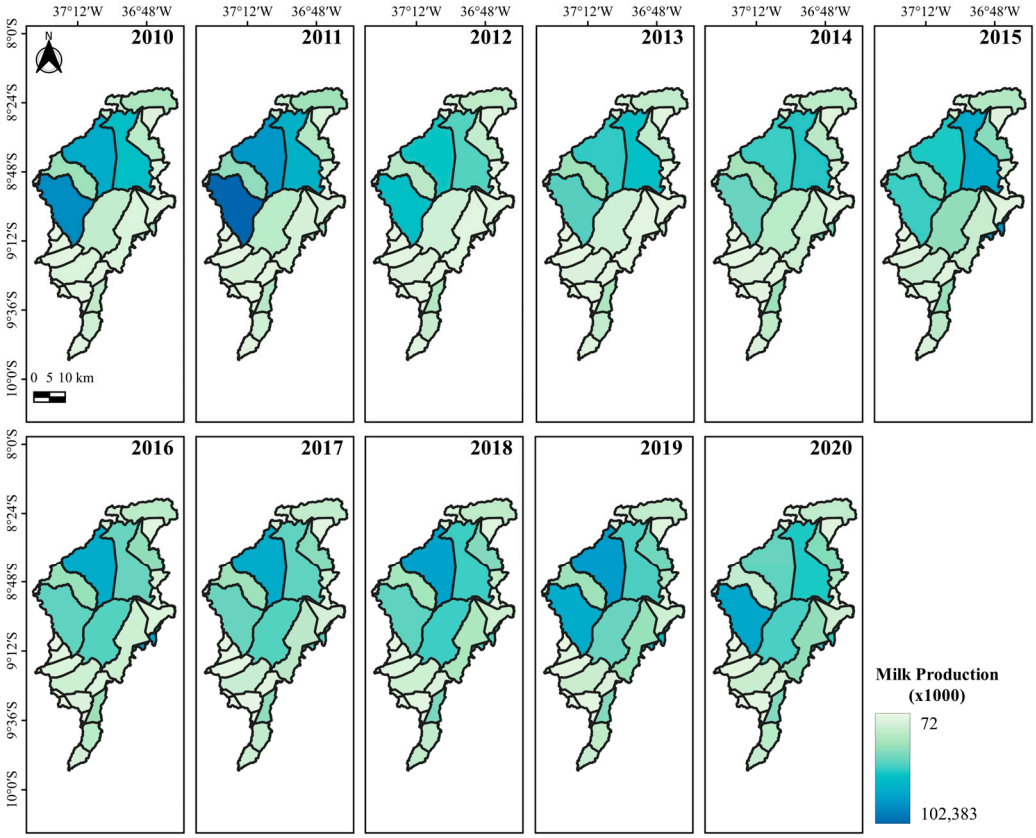

Figure 12. Spatio-temporal dynamics of Milk Production (MP) from 2010 to 2020 in the IRW.

Table 9. Ranking of the five municipalities with the highest MP from 2010 to 2020 in the IRW.

Year	Municipality				
	1°	2°	3°	4°	5°
2010	Itaíba	Buíque	Pedra	Tupanatinga	Pesqueira
2011	Itaíba	Buíque	Pedra	Tupanatinga	Pesqueira
2012	Itaíba	Buíque	Pedra	Major Isidoro	Tupanatinga
2013	Pedra	Buíque	Itaíba	Tupanatinga	Major Isidoro
2014	Pedra	Buíque	Itaíba	Bom Conselho	Major Isidoro
2015	Bom Conselho	Pedra	Buíque	Itaíba	Venturosa
2016	Bom Conselho	Buíque	Águas Belas	Itaíba	Pedra
2017	Buíque	Bom Conselho	Águas Belas	Pedra	Itaíba
2018	Buíque	Pedra	Águas Belas	Bom Conselho	Itaíba
2019	Buíque	Itaíba	Bom Conselho	Pedra	Águas Belas
2020	Itaíba	Pedra	Bom Conselho	Águas Belas	Buíque

When comparing the data presented with the information from the land use and occupation map via MapBiomas (Figure 4) and the LVI (Figures 8 and 9), it can be seen that the municipalities with the highest EH, MC, and MP rankings are located in the Agriculture and Livestock areas in land use and occupation, and in the high vulnerability class in the LVI, corroborating the relationship between all the variables analyzed.

Several studies related to dairy cattle productivity have been conducted in the semi-arid regions of the world, which support the importance of analyzing the data presented here. For instance, Oumou et al. [88] conducted a study on the analysis of milk production systems in the Sahelian zone of Burkina Faso, and Wankar et al. [89] discussed thermal

stress in dairy animals and current trends in milk production, analyzing production in the Americas, Europe, Africa, Oceania, and Asia. They concluded that milk production is under serious threat from global warming and that it is urgent to optimize production systems and mitigate climate risks.

We also highlight the work of Brizga et al. [90], who investigated the environmental impacts of dairy farms in Latvia with different management practices, emphasizing that milk production depends on the diet and the cows' ability to consume dry matter (DM); Froldi et al. [91], on the environmental impacts of milk produced for cheese manufacturing in Northern Italy, concluding that the degree of specialization of dairy farms and proper management reduce the environmental impact. Darré et al. [92], who estimated the global and local environmental impacts per kg of milk and per hectare in a case study in Uruguay, concluding that management factors, including diet type, input amounts, and grazing system type, can be more relevant in determining the environmental impacts of dairy systems than productivity itself. Finally, we highlight the study by Wilkinson et al. [93] on grazing dairy cows, which observed that the carbon footprint is lower in pasture systems compared to other milk production systems, and also noted that health and welfare indicators are positively influenced by extensive grazing practices.

In this regard, we highlight that the lack of knowledge and adequate information is an obstacle to adaptation and, therefore, requires high-quality, accurate, and accessible information [84], such as the analysis conducted here.

3.5. Analysis of the Dynamics of Pasture Cover and Quality

The analysis of Pasture Cover via the Pasture Atlas (Figure 13) shows the amount of pasture in the total area of the municipalities.

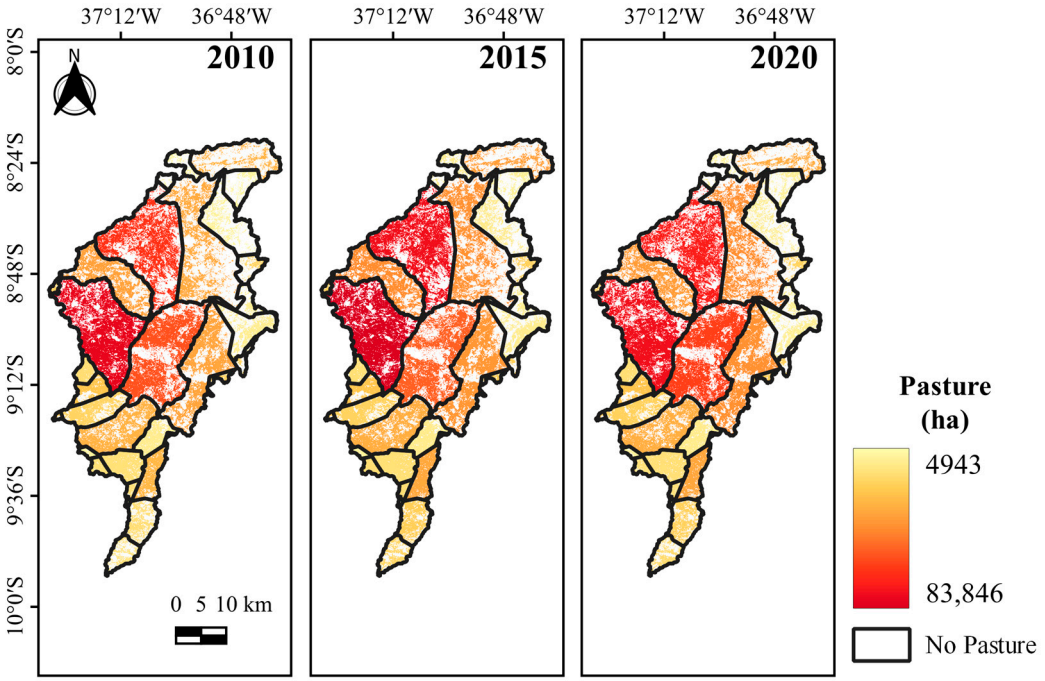

Figure 13. Change at five-year intervals, in spatio-temporal dynamics of the Total Pasture Cover Area of municipalities from 2010 to 2020 in IRW.

There is a further relationship between the values of the largest pasture areas and the parameters of Effective Herd, Milked Cows, and Milk Production (×1000), where the municipality with the largest pasture area was the municipality of Itaíba with a maximum value of 83,846 ha in 2015 and a minimum of 76,067 ha in 2020 (Table 10). From 2010 to 2018, among the five municipalities with the largest pasture areas, Buíque ranked second, with a maximum of 75,984 ha in 2015 and a minimum of 65,709 ha in 2010. In 2019 and

2020, the municipality of Ibimirim was in second place, with 75,555 ha and 75,110 ha, respectively. From 2014 to 2018, it was in third place, and from 2010 to 2013, it was in fourth place. Although the municipality of Ibimirim does not appear in the rankings of municipalities with the highest EH, MC, and MP, it is among the municipalities with the largest pasture areas. This is because, in the last decades, in order to promote a high-productivity agricultural model, governments have invested in water infrastructure to create various irrigation districts, and one of these irrigable sectors is the Moxotó Irrigated Perimeter (Pimox), made up of diversified agricultural systems located downstream of the Eng. Francisco Sabóia Dam, known as the Poço da Cruz Dam, in that municipality [94]. The other municipalities with the largest areas are Águas Belas, Tupanatinga, and Pedra, with maximum values of 63,963 ha in 2019, 44,065 ha in 2015, and 46,026 ha in 2018, respectively.

Table 10. Ranking of the five municipalities with the largest area of pasture cover from 2010 to 2020 in the IRW.

Year	Municipality				
	1°	2°	3°	4°	5°
2010	Itaíba	Buíque	Águas Belas	Ibimirim	Tupanatinga
2011	Itaíba	Buíque	Águas Belas	Ibimirim	Tupanatinga
2012	Itaíba	Buíque	Águas Belas	Ibimirim	Tupanatinga
2013	Itaíba	Buíque	Águas Belas	Ibimirim	Tupanatinga
2014	Itaíba	Buíque	Ibimirim	Águas Belas	Tupanatinga
2015	Itaíba	Buíque	Ibimirim	Águas Belas	Tupanatinga
2016	Itaíba	Buíque	Ibimirim	Águas Belas	Tupanatinga
2017	Itaíba	Buíque	Ibimirim	Águas Belas	Pedra
2018	Itaíba	Buíque	Ibimirim	Águas Belas	Pedra
2019	Itaíba	Ibimirim	Buíque	Águas Belas	Pedra
2020	Itaíba	Ibimirim	Buíque	Águas Belas	Pedra

These data are fundamentally important in the context of maintaining the economic activity of dairy farming, as corroborated by studies such as those by Godde et al. [95], which state that changes in herbaceous vegetation (pasture areas) will have consequences on livestock production, with a decrease in global pastures between 2000 and 2050 posing a challenge for herd management. Similarly, Wróbel et al. [96] evaluated the challenges of pasture-based feeding systems, concluding that among the significant advantages of feeding dairy cows on pastures are the high quality and health benefits of milk and dairy products, which translate into health benefits for consumers.

The Pasture Quality via MapBiomas (Figure 14) showed visually similar data with regard to the Pasture Coverage indicated by the Atlas of Pastures (Figure 13); however, the methodology for classifying areas of Pasture Quality does not present quantitative values by municipality, and is classified qualitatively, so a comparison between the data by municipality area was not carried out. However, Hu et al. [97], in a study on soil structural degradation in New Zealand, concluded that soil structural degradation due to compaction is typically associated with reduced pasture and crop production, where more intensive land uses for dairy cattle grazing resulted in a higher degree of soil structural degradation.

The analysis of Pasture Quality classes allows a comparison between the Severe Degradation, Moderate Degradation, and Not Degraded classes, which can be seen in Table 11.

Areas with Severe Degradation showed increasing values from 2010 to 2014, with a maximum value of 272,222 ha in 2014. From 2015 onwards, there was a gradual decrease in the class, reaching a minimum value of 139,294 ha in 2019 and rising again in 2020. The Moderate Degradation class maintained high average values, with a maximum value of 199,882 ha in 2011 and a minimum value of 150,009 ha in 2010. Finally, the areas in the Not Degraded pasture class were the smallest in the entire classification, with values that

fluctuated, reaching a maximum of 195,328 ha in 2010 and a minimum of 24,260 ha in 2014. Figure 15 shows the variation of the classes regarding the years.

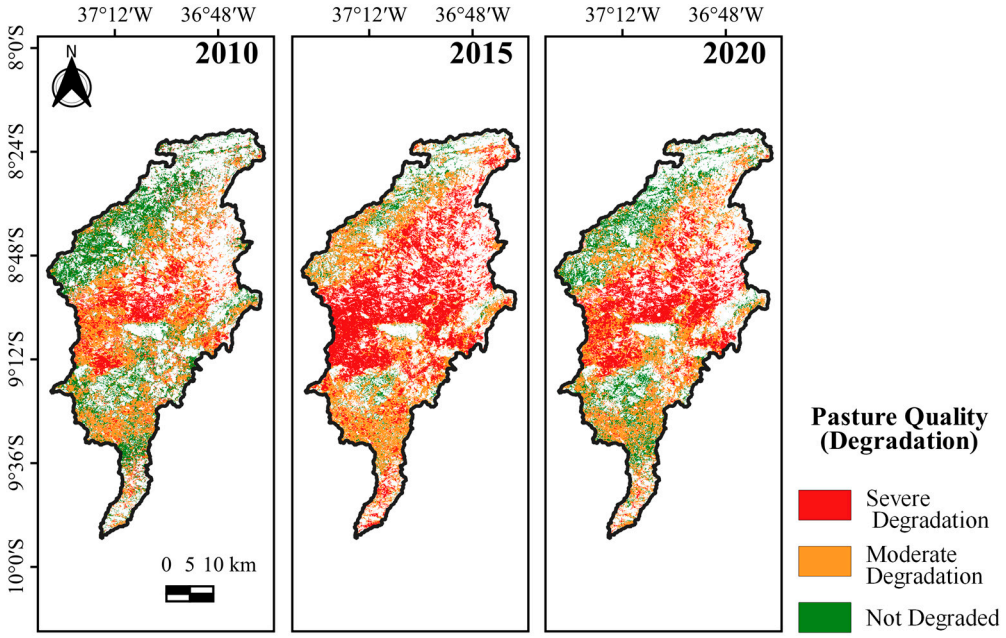

Figure 14. Change, at five-year intervals, in spatio-temporal dynamics of Pasture Quality from 2010 to 2020 in the IRW.

Table 11. Area of Pasture Quality classes from 2010 to 2020 in IRW.

Classes	Area (ha)		
	Severe Degradation	Moderate Degradation	Not Degraded
2010	93,359	150,009	195,328
2011	118,347	199,882	100,442
2012	182,393	185,604	51,579
2013	204,220	173,107	46,250
2014	272,222	152,569	24,260
2015	234,501	192,537	35,032
2016	221,027	183,626	42,873
2017	210,405	175,385	48,414
2018	185,251	190,702	71,657
2019	139,294	192,502	96,151
2020	146,173	197,212	97,255

According to the FAO [98], one of the main causes of pasture degradation under direct anthropogenic influence is inadequate management, in particular, the systematic use of stocking rates that exceed the pasture's ability to recover from grazing and trampling, which justifies, as we can see in the quantification of EH (Figure 10), the fact that the areas representing the Severe Degradation class correspond to the municipalities with the highest EH numbers. Gosch et al. [99] carried out an assessment via Landsat of the quantitative and qualitative dynamics of pasture areas in rural settlements in the state of Goiás, concluding that it was possible to extract information from satellite images efficiently and accurately regarding the pasture quality; however, they emphasized that exploring pasture quality standards via MapBiomas does not present a high accuracy, justifying that the platform uses general standards on pasture quality. The quality and the quantity of pasture were also described by Duguma [100] as critical and limiting factors affecting the dairy production of small-scale farmers and ensuring optimal production.

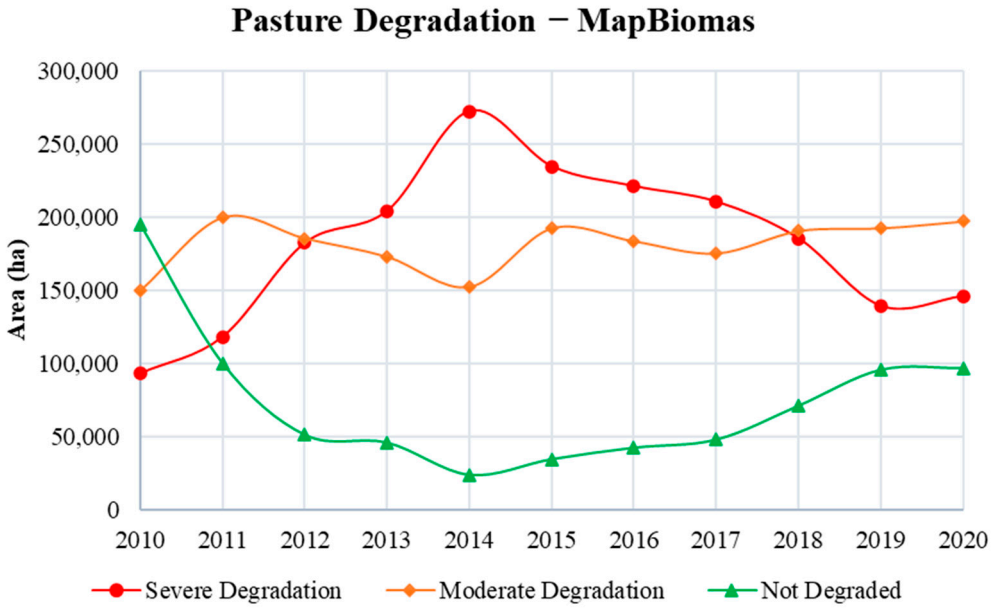

Figure 15. Graphical representation of the area of Pasture Quality classes from 2010 to 2020 in IRW.

3.6. Statistical Analysis

Table 12 presents the multivariate component statistics by principal component (PC), including eigenvalues, total variance, and cumulative variance (%) for all principal components 1 through 8 (PC1 and PC8). The eigenvalues of PC1 and 2 were greater than 1. Therefore, according to the Kaiser [67] criterion, they can be used to generate and interpret the biplot graphs and together they represent more than 70% of the variance in the data.

Table 12. Principal components 1 to 8 (PC1 through PC8) of the variables studied, along with their respective eigenvalues, total variance, and cumulative variance (%).

Dry Season								
	PC(1)	PC(2)	PC(3)	PC(4)	PC(5)	PC(6)	PC(7)	PC(8)
Eigenvalue	4.43	1.76	1.00	0.42	0.21	0.17	0.02	0.00
Total Variance	0.55	0.22	0.12	0.05	0.03	0.02	0.00	0.00
Cumulative variance (%)	55.3%	77.3%	89.8%	95.1%	97.7%	99.8%	100.0%	100.0%
Rainy Season								
	PC(1)	PC(2)	PC(3)	PC(4)	PC(5)	PC(6)	PC(7)	PC(8)
Eigenvalue	4.26	1.91	0.99	0.55	0.21	0.06	0.02	0.00
Total Variance	0.53	0.24	0.12	0.07	0.03	0.01	0.00	0.00
Cumulative variance (%)	53.2%	77.2%	89.6%	96.5%	99.1%	99.8%	100.0%	100.0%

The total variance indicates the representativeness and significance of the data, with 77.3% for the dry period and 77.2% for the rainy period in the cumulative PC2, suggesting the importance of the correlations between the LVI index, the MapBiomas majority classes (five classes), the Effective Herd and Pasture. In a study by Silva et al. [22], applying principal component analysis to monitor soil indicators and pasture production areas, cumulative variances between 50% and 60% were found. This allowed for the extraction of significant information from the correlations between the indices and the establishment of a multiple regression model with satisfactory results. Salvati et al. [101], in a multivariate evaluation of the agroforestry landscape, found a cumulative variance of 52%, Zeraatpisheh et al. [102], using covariance and multivariate statistical analyses in a case study in semiarid regions, found a cumulative variance in the first two components (PCA 1 and PCA 2) that explained more than 42% of the total variability.

In the dry season (Figure 16), there is an inverse correlation between the Forest variable and the "Pasture" and "Agriculture and Livestock" variables. The year 2010 was the most correlated with the Forest variable and the years 2017, 2018, 2019, and 2020 were the most correlated with the "Pasture" and "Agriculture and Livestock" variables. The LVI variable maintained a correlation with the Non-Forest Natural Formation and Non-Vegetated Area variables, which is explained by the fact that the LVI increases with an increase in these variables, and has an inverse correlation with the Forest, Effective Herd, and Water Bodies variables. The years 2013, 2014, 2015, and 2016 are related to the Non-Forest Natural Formation and Non-Vegetated Area classes, and the year 2011 was more related to the Effective Herd and Water Bodies variables, corroborating the data obtained through MapBiomas (Figures 5 and 6) and the temporal analysis of Effective Herd (Figure 10), as well as greater contributions in the years 2013 and 2017 from the Non-Forest Natural Formation, Non-Vegetated Area, and Agriculture and Livestock classes.

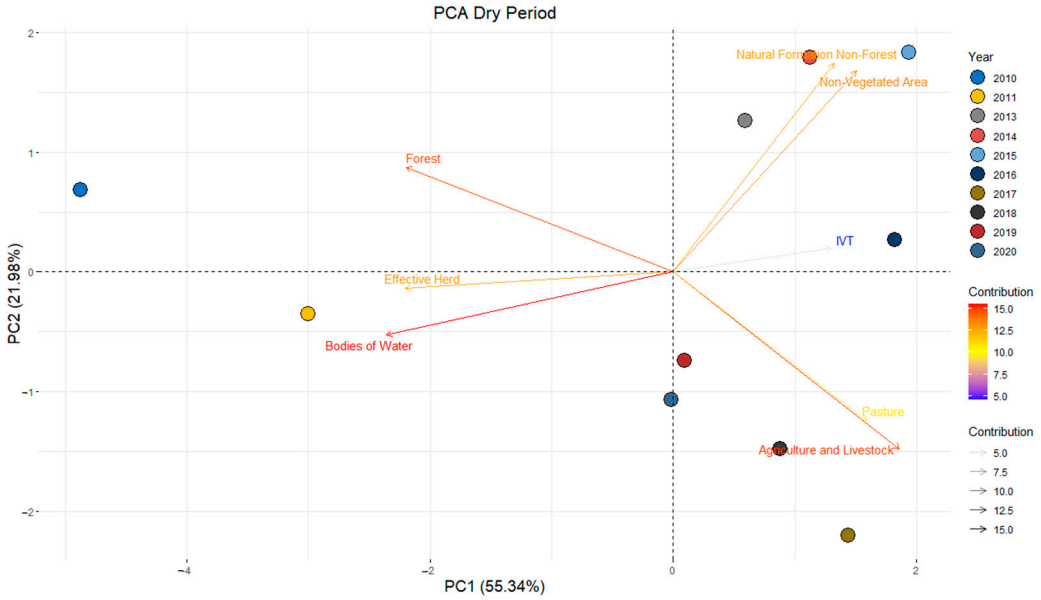

Figure 16. Principal component analysis of the variables of the Land Vulnerability Index (LVI), the majority classes of MapBiomas (five classes), the Effective Herd and Pasture for the dry period of the years 2010 to 2020 in IRW.

Figure 17 shows a strong correlation between all the variables ($R^2 > 0.8$), except for the variables Pasture and LVI, which showed relatively low correlations ($R^2 < 0.6$).

For the rainy season (Figure 18), the Forest and LVI variables were inversely correlated with the Pasture and Agriculture and Livestock variables, with the Forest variable being representative in 2011. The Non-Forest Natural Formation and Non-Vegetated Area variables also maintained a strong correlation with each other and an inverse correlation with the Effective Herd and Water Bodies variables. The year 2010 was more representative for the Effective Herd and Water Bodies variables. The years 2013 to 2016 for Non-Forest Natural Formation and Non-Vegetated Area and the years 2017 to 2020 for Pasture and Agriculture and Livestock, corroborating the data provided by MapBiomas (Figures 5 and 6) and the temporal analysis of Effective Herd (Figure 10).

The correlation remained high ($R^2 > 0.8$) between most of the variables (Figure 19), except for the Non-Forest Natural Formation and Pasture variables ($0.6 < R^2 < 0.7$) and the LVI, which showed the lowest correlation ($R^2 < 0.5$).

Given the context presented, it is evident that over the 10-year study period (2010–2020), the dairy basins of Pernambuco and Alagoas, which are part of the IRW, showed a strong process of degradation, with significant losses of the native vegetation of the Caatinga Biome and an increase in pasture areas and land vulnerability. Similar results were found

by Silva et al. [103], who analyzed a 20-year time series (1998–2018) and identified that the primary driver of soil and vegetation degradation in the region was largely associated with the expansion of pasture areas to support dairy farming and by Melo et al. [72] who noted that between 2017 and 2020, soil and vegetation degradation occurred in certain areas of the dairy basin region in the state of Pernambuco.

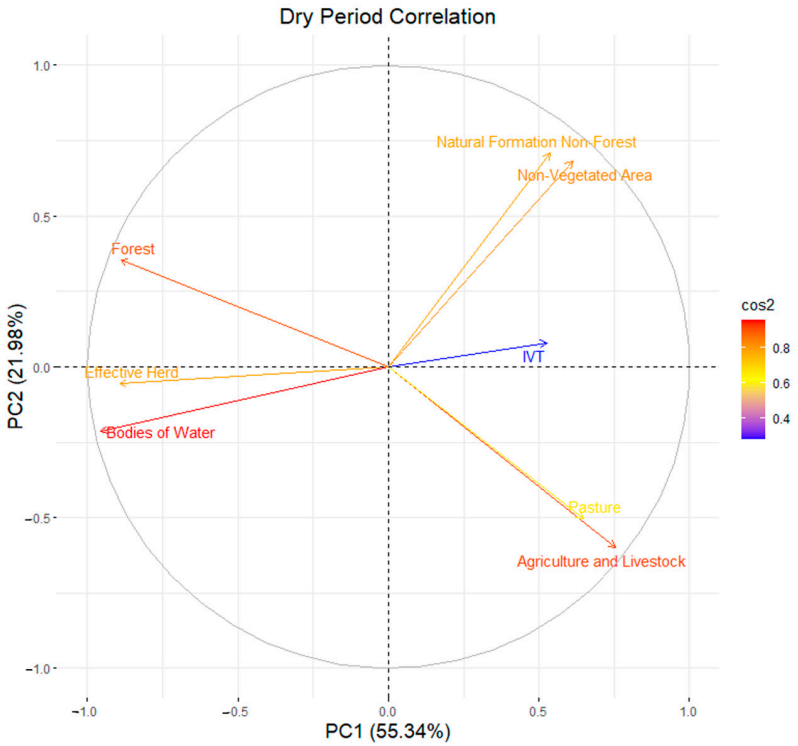

Figure 17. Correlation of the principal components of the variables Land Vulnerability Index (LVI), the MapBiomas majority classes (five classes), and the Effective Herd and Pasture for the dry period from 2010 to 2020 in IRW.

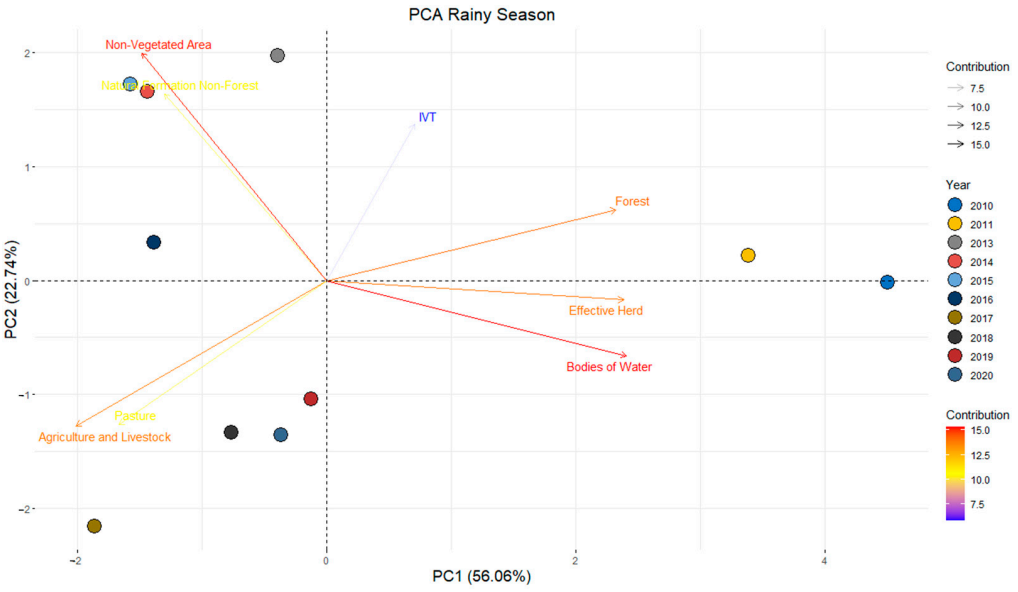

Figure 18. Principal component analysis of the variables NDVI, IVV, IBVL, and LVI*, the MapBiomas majority classes (five classes), and the Effective Herd for the rainy season from 2010 to 2020 in IRW. Note: NDVI = Normalized Difference Vegetation Index; IVV = Vegetation Vulnerability Index; IBVL = Woody Vegetation Biomass Index; LVI = Land Vulnerability Index.

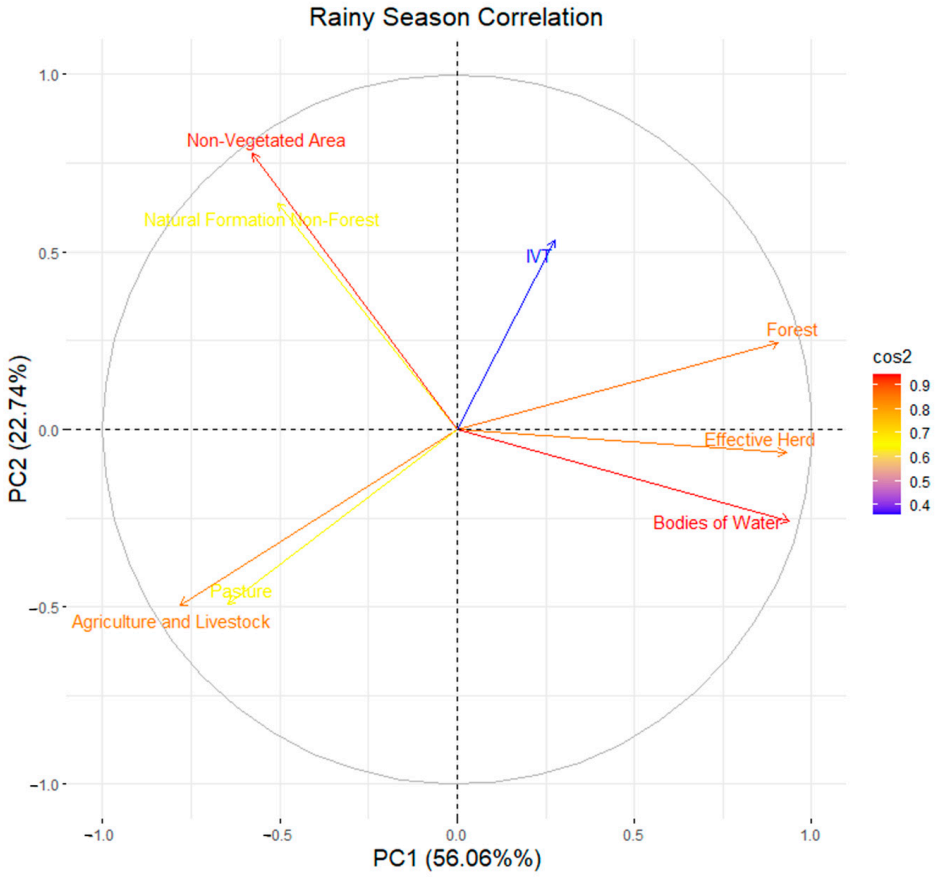

Figure 19. Correlation of the principal components of the variables NDVI, IVV, IBVL, and LVI*, the MapBiomas majority classes (five classes), and the Effective Herd for the rainy season from 2010 to 2020 in IRW. Note: NDVI = Normalized Difference Vegetation Index; IVV = Vegetation Vulnerability Index; IBVL = Woody Vegetation Biomass Index; LVI = Land Vulnerability Index.

4. Conclusions

The study reveals a reduction in native vegetation in the Caatinga Biome, with a significant increase in areas dedicated to agriculture, livestock, and pastures. This phenomenon is associated with degradation processes caused by anthropogenic actions and exacerbated by drought periods. The spatial and temporal analysis of dairy basins in Pernambuco and Alagoas, within the Ipanema River Watershed, showed an expansion of pasture areas, highlighting soil vulnerability and the need for sustainable management practices.

The information generated is crucial for formulating public policies aimed at reducing environmental degradation and promoting agricultural sustainability in semiarid regions. Remote sensing and geoprocessing technologies used in the study proved effective for continuous land use monitoring, contributing to natural resource conservation and sustainable economic development.

Future studies should expand the analysis to other river basins and incorporate new remote sensing technologies and predictive modeling techniques. Additionally, exploring sustainable soil and water management practices is important to mitigate degradation and promote the recovery of affected areas.

Author Contributions: Conceptualization, J.B.A.d.S., G.L.P.d.A., M.V.d.S., H.P., C.G. and M.B.F.; methodology, J.B.A.d.S., G.L.P.d.A., M.V.d.S., J.F.d.O.-J., C.G., I.A.B. and M.B.F.; software, J.B.A.d.S., M.V.d.S. and P.R.G.; validation, J.B.A.d.S., M.V.d.S. and I.A.B.; formal analysis, J.B.A.d.S. and G.A.P.d.A.M.; investigation, J.B.A.d.S.; resources, M.V.d.S. and J.F.d.O.-J.; data curation, M.V.d.S., P.R.G. and M.B.F.; writing—original draft preparation, J.B.A.d.S., G.L.P.d.A., M.V.d.S., H.P. and G.T.B.M.; writing—review and editing, J.B.A.d.S., G.L.P.d.A., M.V.d.S., J.F.d.O.-J., H.P., P.R.G., G.A.P.d.A.M., C.G., G.T.B.M., I.A.B. and M.B.F.; visualization,

G.L.P.d.A., J.F.d.O.-J., H.P., P.R.G., G.A.P.d.A.M., C.G., G.T.B.M., I.A.B. and M.B.F.; supervision, G.L.P.d.A.; project administration, G.L.P.d.A. and M.V.d.S.; funding acquisition, M.V.d.S. and J.F.d.O.-J. All authors have read and agreed to the published version of the manuscript.

Funding: This research received no external funding.

Data Availability Statement: The data used in this research are confidential and copyright of the authors.

Acknowledgments: To the Programa de Pós-Graduação em Engenharia Agrícola (PGEA) and the Grupo de Pesquisa em Ambiência (GPESA) of the Universidade Federal Rural de Pernambuco (UFRPE) for supporting the development of this research. The Coordenação de Aperfeiçoamento de Pessoal de Nível Superior (CAPES—Finance Code 001) and the Fundação de Amparo à Ciência e Tecnologia do Estado de Pernambuco (FACEPE), for the financing of scholarships.

Conflicts of Interest: The authors declare no conflicts of interest.

References

1. IPCC. The Intergovernmental Panel on Climate Change. Available online: https://www.ipcc.ch/ (accessed on 31 August 2023).
2. Huang, J.; Ji, M.; Xie, Y.; Wang, S.; He, Y.; Ran, J. Global Semi-Arid Climate Change over Last 60 Years. *Clim. Dyn.* **2016**, *46*, 1131–1150. [CrossRef]
3. Stavi, I.; Pinho, J.R.; Paschalidou, A.K.; Adamo, S.B.; Galvin, K.; Sherbinin, A.; Even, T.; Heaviside, C.; van der Geest, K. Food Security among Dryland Pastoralists and Agropastoralists: The Climate, Land-Use Change, and Population Dynamics Nexus. *Anthr. Rev.* **2022**, *9*, 299–323. [CrossRef]
4. Burney, J.; Cesano, D.; Russell, J.; La Rovere, E.L.; Corral, T.; Coelho, N.S.; Santos, L. Climate Change Adaptation Strategies for Smallholder Farmers in the Brazilian Sertão. *Clim. Chang.* **2014**, *126*, 45–59. [CrossRef]
5. Oliveira, M.L.; Santos, C.A.C.; Oliveira, G.; Perez-Marin, A.M.; Santos, C.A.G. Effects of Human-Induced Land Degradation on Water and Carbon Fluxes in Two Different Brazilian Dryland Soil Covers. *Sci. Total Environ.* **2021**, *792*, 148458. [CrossRef] [PubMed]
6. Andrade, C.W.L.; Montenegro, S.M.G.L.; Montenegro, A.A.A.; Lima, J.R.S.; Srinivasan, R.; Jones, C.A. Climate Change Impact Assessment on Water Resources under RCP Scenarios: A Case Study in Mundaú River Basin, Northeastern Brazil. *Int. J. Climatol.* **2021**, *41*, E1045–E1061. [CrossRef]
7. Maranhão, S.R.; Silva, R.G.; Araújo, G.G.L.; Cândido, M.J.D. Modeling the Water Balance of a Ruminant Production System in the Semi-Arid Region. *Afr. J. Agric. Res.* **2022**, *18*, 127–135. [CrossRef]
8. Medeiros, S.S. *Estabelecimentos Agropecuários do Semiárido Brasileiro*, 1st ed.; Instituto Nacional do Semiárido: Campina Grande, Brazil, 2018.
9. Silva, J.L.B.; Moura, G.B.A.; Silva, M.V.; Lopes, P.M.O.; Guedes, R.V.S.; Silva, Ê.F.F.; Ortiz, P.F.S.; Rodrigues, J.A.M. Changes in the Water Resources, Soil Use and Spatial Dynamics of Caatinga Vegetation Cover over Semiarid Region of the Brazilian Northeast. *Remote Sens. Appl.* **2020**, *20*, 100372. [CrossRef]
10. Vieira, R.M.D.S.P.; Tomasella, J.; Barbosa, A.A.; Martins, M.A.; Rodriguez, D.A.; Rezende, F.S.D.; Carriello, F.; Santana, M.D.O. Desertification Risk Assessment in Northeast Brazil: Current Trends and Future Scenarios. *Land Degrad. Dev.* **2021**, *32*, 224–240. [CrossRef]
11. Queiroz, M.G.; Silva, T.G.F.; Zolnier, S.; Jardim, A.M.R.F.; Souza, C.A.A.; Araújo Júnior, G.N.; Morais, J.E.F.; Souza, L.S.B. Spatial and Temporal Dynamics of Soil Moisture for Surfaces with a Change in Land Use in the Semi-Arid Region of Brazil. *Catena* **2020**, *188*, 104457. [CrossRef]
12. Althoff, T.D.; Menezes, R.S.C.; Pinto, A.S.; Pareyn, F.G.C.; Carvalho, A.L.; Martins, J.C.R.; Carvalho, E.X.; Silva, A.S.A.; Dutra, E.D.; Sampaio, E.V.S.B. Adaptation of the Century Model to Simulate C and N Dynamics of Caatinga Dry Forest before and after Deforestation. *Agric. Ecosyst. Environ.* **2018**, *254*, 26–34. [CrossRef]
13. Fernandes, M.M.; Fernandes, M.R.M.; Garcia, J.R.; Matricardi, E.A.T.; Lima, A.H.S.; Filho, R.N.A.; Filho, R.R.G.; Piscoya, V.C.; Piscoya, T.O.F.; Filho, M.C. Land Use and Land Cover Changes and Carbon Stock Valuation in the São Francisco River Basin, Brazil. *Environ. Chall.* **2021**, *5*, 100247. [CrossRef]
14. Medeiros, A.S.; Maia, S.M.F.; Santos, T.C.; Gomes, T.C.A. Soil Carbon Losses in Conventional Farming Systems Due to Land-Use Change in the Brazilian Semi-Arid Region. *Agric. Ecosyst. Environ.* **2020**, *287*, 106690. [CrossRef]
15. Campos, S.A.C.; Ferreira, M.D.P.; Coelho, A.B.; Lima, J.E. Degradação Ambiental Agropecuária No Bioma Caatinga. *Rev. Econ. Nordeste* **2016**, *46*, 155–170. [CrossRef]
16. Naorem, A.; Jayaraman, S.; Dang, Y.P.; Dalal, R.C.; Sinha, N.K.; Rao, C.S.; Patra, A.K. Soil Constraints in an Arid Environment—Challenges, Prospects, and Implications. *Agronomy* **2023**, *13*, 220. [CrossRef]
17. Balmford, A.; Amano, T.; Bartlett, H.; Chadwick, D.; Collins, A.; Edwards, D.; Field, R.; Garnsworthy, P.; Green, R.; Smith, P.; et al. The Environmental Costs and Benefits of High-Yield Farming. *Nat. Sustain.* **2018**, *1*, 477–485. [CrossRef]

18. Britt, J.H.; Cushman, R.A.; Dechow, C.D.; Dobson, H.; Humblot, P.; Hutjens, M.F.; Jones, G.A.; Mitloehner, F.M.; Ruegg, P.L.; Sheldon, I.M.; et al. Review: Perspective on High-Performing Dairy Cows and Herds. *Animal* **2021**, *15*, 100298. [CrossRef] [PubMed]
19. von Keyserlingk, M.A.G.; Martin, N.P.; Kebreab, E.; Knowlton, K.F.; Grant, R.J.; Stephenson, M.; Sniffen, C.J.; Harner, J.P.; Wright, A.D.; Smith, S.I. Invited Review: Sustainability of the US Dairy Industry. *J. Dairy Sci.* **2013**, *96*, 5405–5425. [CrossRef]
20. Neethirajan, S. Innovative Strategies for Sustainable Dairy Farming in Canada amidst Climate Change. *Sustainability* **2023**, *16*, 265. [CrossRef]
21. Dias Filho, M.B. *Diagnóstico Das Pastagens No Brasil*; Embrapa Amazônia Oriental, Ed.; Embrapa Amazônia Oriental: Belém, Brazil, 2014; Volume 1.
22. Silva, M.V.; Pandorfi, H.; Almeida, G.L.P.; Lima, R.P.; Santos, A.; Jardim, A.M.R.F.; Rolim, M.M.; Silva, J.L.B.; Batista, P.H.D.; Silva, R.A.B.; et al. Spatio-Temporal Monitoring of Soil and Plant Indicators under Forage Cactus Cultivation by Geoprocessing in Brazilian Semi-Arid Region. *J. S. Am. Earth Sci.* **2021**, *107*, 103155. [CrossRef]
23. IBGE. Censo Agro. 2017. Available online: https://censos.ibge.gov.br/agro/2017/templates/censo_agro/resultadosagro/pecuaria.html?localidade=0&tema=75657 (accessed on 21 August 2023).
24. Batista, P.H.D.; Almeida, G.L.P.; Silva, J.L.B.; Pandorfi, H.; Silva, M.V.; Silva, R.A.B.; Melo, M.V.N.; Lins, F.A.C.; Cordeiro, J.J.F., Jr. Short-Term Grazing and Its Impacts on Soil and Pasture Degradation. *Dyna* **2020**, *87*, 123–128. [CrossRef]
25. Bolfe, É.L.; Victoria, D.C.; Sano, E.E.; Bayma, G.; Massruhá, S.M.F.S.; Oliveira, A.F. Potential for Agricultural Expansion in Degraded Pasture Lands in Brazil Based on Geospatial Databases. *Land* **2024**, *13*, 200. [CrossRef]
26. Andrade, T.S.; Cunha, J.E.B.L.; Galvão, C.O.; Rufino, I.A.A. Milk Production as an Indicator of Drought Vulnerability of Cities Located in the Brazilian Semiarid Region. *Eng. Agrícola* **2017**, *37*, 1203–1212. [CrossRef]
27. Feltran-Barbieri, R.; Féres, J.G. Degraded Pastures in Brazil: Improving Livestock Production and Forest Restoration. *R. Soc. Open Sci.* **2021**, *8*, 201854. [CrossRef] [PubMed]
28. Muralikrishnan, L.; Padaria, R.N.; Choudhary, A.K.; Dass, A.; Shokralla, S.; El-Abedin, T.K.Z.; Abdelmohsen, S.A.M.; Mahmoud, E.A.; Elansary, H.O. Climate Change-Induced Drought Impacts, Adaptation and Mitigation Measures in Semi-Arid Pastoral and Agricultural Watersheds. *Sustainability* **2021**, *14*, 6. [CrossRef]
29. Weng, C.; Bai, Y.; Chen, B.; Hu, Y.; Shu, J.; Chen, Q.; Wang, P. Assessing the Vulnerability to Climate Change of a Semi-Arid Pastoral Social–Ecological System: A Case Study in Hulunbuir, China. *Ecol. Inf.* **2023**, *76*, 102139. [CrossRef]
30. Ndiritu, S.W. Drought Responses and Adaptation Strategies to Climate Change by Pastoralists in the Semi-Arid Area, Laikipia County, Kenya. *Mitig. Adapt. Strat. Glob. Chang.* **2021**, *26*, 10. [CrossRef]
31. Fust, P.; Schlecht, E. Importance of Timing: Vulnerability of Semi-Arid Rangeland Systems to Increased Variability in Temporal Distribution of Rainfall Events as Predicted by Future Climate Change. *Ecol. Model.* **2022**, *468*, 109961. [CrossRef]
32. Nandintsetseg, B.; Boldgiv, B.; Chang, J.; Ciais, P.; Davaanyam, E.; Batbold, A.; Bat-Oyun, T.; Stenseth, N.C. Risk and Vulnerability of Mongolian Grasslands under Climate Change. *Environ. Res. Lett.* **2021**, *16*, 034035. [CrossRef]
33. Pereira, P.; Bogunovic, I. Land Degradation Neutrality. How to Reverse Land Degradation with Conservation Agriculture Practices. In Proceedings of the 12th International Scientific/Professional Conference Agriculture in Nature and Environment Protection, Osijek, Croatia, 7–9 September 2019; pp. 27–29.
34. Gibbs, H.K.; Salmon, J.M. Mapping the World's Degraded Lands. *Appl. Geogr.* **2015**, *57*, 12–21. [CrossRef]
35. Zhou, N.; Hu, X.; Byskov, I.; Næss, J.S.; Wu, Q.; Zhao, W.; Cherubini, F. Overview of Recent Land Cover Changes, Forest Harvest Areas, and Soil Erosion Trends in Nordic Countries. *Geogr. Sustain.* **2021**, *2*, 163–174. [CrossRef]
36. MAPBIOMAS BRASIL. Plataforma de Mapas e Dados. Available online: http://plataforma.mapbiomas.org/map (accessed on 20 October 2023).
37. Alvares, C.A.; Stape, J.L.; Sentelhas, P.C.; Gonçalves, J.L.M.; Sparovek, G. Köppen's Climate Classification Map for Brazil. *Meteorol. Z.* **2013**, *22*, 711–728. [CrossRef]
38. Beck, H.E.; Zimmermann, N.E.; McVicar, T.R.; Vergopolan, N.; Berg, A.; Wood, E.F. Present and Future Köppen-Geiger Climate Classification Maps at 1-Km Resolution. *Sci. Data* **2018**, *5*, 180214. [CrossRef]
39. INMET. Dados Históricos Anuais. Available online: https://portal.inmet.gov.br/dadoshistoricos (accessed on 25 August 2023).
40. INMET. Normais Climatológicas Do Brasil. Available online: https://portal.inmet.gov.br/normais (accessed on 26 August 2023).
41. FAO. *OECD-FAO Agricultural Outlook 2020–2029*, 1st ed.; Paris/FAO, Ed.; OECD: Rome, Italy, 2020; Volume 1, ISBN 9789264317673.
42. Agrofy News Quem São Os Maiores Produtores de Leite Do Mundo? | Agrofy News. Available online: https://news.agrofy.com.br/noticia/201002/quem-sao-os-maiores-produtores-leite-do-mundo (accessed on 28 July 2024).
43. *Embrapa Lei Baixo Carbono*; Embrapa Brazilian Agricultural Research Corporation: Brasília, Brazil, 2023.
44. IBGE. Panorama Brasil. Available online: https://cidades.ibge.gov.br/brasil/panorama (accessed on 21 August 2023).
45. Wu, Z.; Du, Y.; Yang, G.; Lin, L.; Hou, X.; Tan, Y.; Fan, X.; Ren, Y.; Wu, B.; Liu, S.; et al. Improving the Sustainability of Milk Production across Different Climate Regions in China. *Sustain. Prod. Consum.* **2024**, *49*, 446–461. [CrossRef]
46. Bórawski, P.; Pawlewicz, A.; Parzonko, A.; Harper, J.K.; Holden, L. Factors Shaping Cow's Milk Production in the EU. *Sustainability* **2020**, *12*, 420. [CrossRef]
47. Barreto, J.B.; Silva, J.B.; Araújo, S.M.S.; Teixeira, R.O. Análise Do Sistema de Validação e Refinamento de Alertas Do Mapbiomas e Do Laudo de Área Desmatada Em Altamira—PA, Brasil (2018–2021). *Res. Soc. Dev.* **2021**, *10*, e37810615801. [CrossRef]

48. Marengo, J.A.; Alves, L.M.; Alvala, R.C.S.; Cunha, A.P.; Brito, S.; Moraes, O.L.L. Climatic Characteristics of the 2010-2016 Drought in the Semiarid Northeast Brazil Region. *Acad. Bras. Cienc.* **2018**, *90*, 1973–1985. [CrossRef]
49. Santos, A.; Lopes, P.M.O.; Silva, M.V.; Jardim, A.M.R.F.; Moura, G.B.A.; Fernandes, G.S.T.; Silva, D.A.O.; Silva, J.L.B.; Rodrigues, J.A.M.; Silva, E.A.; et al. Causes and Consequences of Seasonal Changes in the Water Flow of the São Francisco River in the Semiarid of Brazil. *Environ. Sustain. Indic.* **2020**, *8*, 100084. [CrossRef]
50. NASA. Landsat Science. Available online: https://landsat.gsfc.nasa.gov/ (accessed on 28 July 2024).
51. Kumar, B.P.; Babu, K.R.; Anusha, B.N.; Rajasekhar, M. Geo-Environmental Monitoring and Assessment of Land Degradation and Desertification in the Semi-Arid Regions Using Landsat 8 OLI/TIRS, LST, and NDVI Approach. *Environ. Chall.* **2022**, *8*, 100578. [CrossRef]
52. Hu, Y.; Raza, A.; Syed, N.R.; Acharki, S.; Ray, R.L.; Hussain, S.; Dehghanisanij, H.; Zubair, M.; Elbeltagi, A. Land Use/Land Cover Change Detection and NDVI Estimation in Pakistan's Southern Punjab Province. *Sustainability* **2023**, *15*, 3572. [CrossRef]
53. Yasin, M.Y.; Abdullah, J.; Noor, N.M.; Yusoff, M.M.; Noor, N.M. Landsat Observation of Urban Growth and Land Use Change Using NDVI and NDBI Analysis. *IOP Conf. Ser. Earth Environ. Sci.* **2022**, *1067*, 012037. [CrossRef]
54. USGS/NASA. Landsat Satellite Missions. Available online: https://www.usgs.gov/landsat-missions/landsat-satellite-missions (accessed on 13 December 2022).
55. Silva, J.L.B.; Refati, D.C.; Lima, R.C.C.; Carvalho, A.A.; Ferreira, M.B.; Pandorfi, H.; Silva, M.V. Techniques of Geoprocessing via Cloud in Google Earth Engine Applied to Vegetation Cover and Land Use and Occupation in the Brazilian Semiarid Region. *Geographies* **2022**, *2*, 593–608. [CrossRef]
56. von Keyserlingk, J.; Thieken, A.; Paton, E. Approaches to Assess Land Degradation Risk: A Synthesis. *Ecol. Soc.* **2023**, *28*, art53. [CrossRef]
57. Lopes, I.C.P.; Campos, J.A. Capacidade de Uso Da Terra Da Sub-Bacia Do Córrego Maria Comprida Usando Sistemas de Informações Geográficas. *J. Environ. Anal. Prog.* **2019**, *4*, 110–121. [CrossRef]
58. Embrapa. *Sistema Brasileiro de Classificação de Solos*, 2nd ed.; Embrapa Solos, Ed.; Embrapa: Rio de Janeiro, Brazil, 2006; ISBN 8585864192.
59. Rouse, J.W.; Haas, R.H.; Schell, J.A.; Deering, D.W. Monitoring Vegetation Systems in the Great Plains with ERTS. In *Earth Resources Technology Satellite-1 Symposium*; NASA: Washington, DC, USA, 1973; Volume 1, pp. 309–317.
60. Allen, R.G.; Tasumi, M.; Trezza, R.; Waters, R.; Bastiaanssen, W. SEBAL (Surface Energy Balance Algorithms for Land). In *Advanced Training and Users Manual*; Idaho Implementation; University of Idaho: Moscow, ID, USA, 2002; Volume 1, 97p.
61. Chaves, I.B.; Lopes, V.L.; Folliott, P.F.; Paes-Silva, A.P. Uma Classificação Morfo-Estrutural Para Descrição e Avaliação Da Biomassa Da Vegetação Da Caatinga. *Rev. Caatinga* **2008**, *21*, 204–213.
62. Weishaupt, A.; Ekardt, F.; Garske, B.; Stubenrauch, J.; Wieding, J. Land Use, Livestock, Quantity Governance, and Economic Instruments—Sustainability Beyond Big Livestock Herds and Fossil Fuels. *Sustainability* **2020**, *12*, 2053. [CrossRef]
63. Hennessy, D.; Delaby, L.; van den Pol-van Dasselaar, A.; Shalloo, L. Increasing Grazing in Dairy Cow Milk Production Systems in Europe. *Sustainability* **2020**, *12*, 2443. [CrossRef]
64. Wilkinson, J.M.; Lee, M.R.F.; Rivero, M.J.; Chamberlain, A.T. Some Challenges and Opportunities for Grazing Dairy Cows on Temperate Pastures. *Grass Forage Sci.* **2020**, *75*, 1–17. [CrossRef]
65. LAPIG/UFG. Áreas de Pastagem. Available online: https://atlasdaspastagens.ufg.br/assets/hotsite/documents/metodos/pt/%C3%81rea%20de%20Pastagem.pdf (accessed on 4 September 2023).
66. MAPBIOMAS BRASIL Pastagens Brasileiras Ocupam Área Equivalente a Todo o Estado Do Amazonas. Available online: https://mapbiomas.org/pastagens-brasileiras-ocupam-area-equivalente-a-todo-o-estado-do-amazonas (accessed on 27 October 2023).
67. Kaiser, H.F. The Varimax Criterion for Analytic Rotation in Factor Analysis. *Psychometrika* **1958**, *23*, 187–200. [CrossRef]
68. Silva, M.V.; Pandorfi, H.; Oliveira-Júnior, J.F.; Silva, J.L.B.; Almeida, G.L.P.; Montenegro, A.A.A.; Mesquita, M.; Ferreira, M.B.; Santana, T.C.; Marinho, G.T.B.; et al. Remote Sensing Techniques via Google Earth Engine for Land Degradation Assessment in the Brazilian Semiarid Region, Brazil. *J. S. Am. Earth Sci.* **2022**, *120*, 104061. [CrossRef]
69. R Core Team. R: A Language and Environment for Statistical Computing. Available online: https://www.r-project.org/ (accessed on 6 February 2023).
70. Barreto-Garcia, P.A.B.; Batista, S.G.M.; Gama-Rodrigues, E.F.; Paula, A.; Batista, W.C.A. Short-Term Effects of Forest Management on Soil Microbial Biomass and Activity in Caatinga Dry Forest, Brazil. *Ecol. Manag.* **2021**, *481*, 118790. [CrossRef]
71. Fernandes, M.M.; Fernandes, M.R.M.; Garcia, J.R.; Matricardi, E.A.T.; Almeida, A.Q.; Pinto, A.S.; Menezes, R.S.C.; Silva, A.J.; Lima, A.H.S. Assessment of Land Use and Land Cover Changes and Valuation of Carbon Stocks in the Sergipe Semiarid Region, Brazil: 1992–2030. *Land Use Policy* **2020**, *99*, 104795. [CrossRef]
72. Melo, M.V.N.; Oliveira, M.E.G.; Almeida, G.L.P.; Gomes, N.F.; Morales, K.R.M.; Santana, T.C.; Silva, P.C.; Moraes, A.S.; Pandorfi, H.; Silva, M.V. Spatiotemporal Characterization of Land Cover and Degradation in the Agreste Region of Pernambuco, Brazil, Using Cloud Geoprocessing on Google Earth Engine. *Remote Sens. Appl.* **2022**, *26*, 100756. [CrossRef]
73. MAPBIOMAS BRASIL. Análise de Acurácia. Available online: https://mapbiomas.org/analise-de-acuracia (accessed on 5 November 2023).
74. Sousa Júnior, V.P.; Sparacino, J.; Espindola, G.M.; Sousa de Assis, R.J. Land-Use and Land-Cover Dynamics in the Brazilian Caatinga Dry Tropical Forest. *Conservation* **2022**, *2*, 739–752. [CrossRef]

75. So, H.B.; Khalifa, A.M.; Yu, B.; Caroll, C.; Burger, P.; Mulligan, D. MINErosion 3: Using Measurements on a Tilting Flume-Rainfall Simulator Facility to Predict Erosion Rates from Post-Mining Landscapes in Central Queensland, Australia. *PLoS ONE* **2018**, *13*, e0194230. [CrossRef]
76. Brasil Lei No 12.727, de 17 de Outubro de 2012. Available online: https://www.planalto.gov.br/ccivil_03/_ato2011-2014/2012/lei/l12727.htm (accessed on 19 June 2023).
77. Tolche, A.D.; Gurara, M.A.; Pham, Q.B.; Anh, D.T. Modelling and Accessing Land Degradation Vulnerability Using Remote Sensing Techniques and the Analytical Hierarchy Process Approach. *Geocarto Int.* **2022**, *37*, 7122–7142. [CrossRef]
78. Hossain, A.; Krupnik, T.J.; Timsina, J.; Mahboob, M.G.; Chaki, A.K.; Farooq, M.; Bhatt, R.; Fahad, S.; Hasanuzzaman, M. Agricultural Land Degradation: Processes and Problems Undermining Future Food Security. In *Environment, Climate, Plant and Vegetation Growth*; Springer International Publishing: Cham, Switzerland, 2020; pp. 17–61.
79. Duguma, B.; Janssens, G.P.J. Assessment of Livestock Feed Resources and Coping Strategies with Dry Season Feed Scarcity in Mixed Crop–Livestock Farming Systems around the Gilgel Gibe Catchment, Southwest Ethiopia. *Sustainability* **2021**, *13*, 10713. [CrossRef]
80. Cantalice, J.R.B.; Nunes, E.O.S.; Cavalcante, D.M.; Barbosa, B.; Barros Junior, G.; Guerra, S.M.S.; Rolim Neto, F.C. Vegetative-Hydraulic Parameters Generated by Agricultural Crops for Laminar Flows under a Semi-Arid Environment of Pernambuco, Brazil. *Ecol. Indic.* **2019**, *106*, 105496. [CrossRef]
81. Almeida, R.F. Palma Forrageira na Alimentação de Ovinos e Caprinos No Semi-Árido Brasileiro. *Rev. Verde Agroecol. Desenvolv. Sustentável* **2012**, *7*, 08–14.
82. Silva, J.B.A.; Almeida, G.L.P.; Silva, M.V.; Oliveira-Junior, J.F.; Pandorfi, H.; Sousa, A.M.O.; Marinho, G.T.B.; Giongo, P.R.; Ferreira, M.B.; Sousa, J.S.; et al. Characterization of Water Status and Vegetation Cover Change in a Watershed in Northeastern Brazil. *J. S. Am. Earth Sci.* **2023**, *130*, 104546. [CrossRef]
83. Silva, J.L.B.; Moura, G.B.A.; Silva, M.V.; Oliveira-Júnior, J.F.; Jardim, A.M.R.F.; Refati, D.C.; Lima, R.C.C.; Carvalho, A.A.; Ferreira, M.B.; Brito, J.I.B.; et al. Environmental Degradation of Vegetation Cover and Water Bodies in the Semiarid Region of the Brazilian Northeast via Cloud Geoprocessing Techniques Applied to Orbital Data. *J. S. Am. Earth Sci.* **2023**, *121*, 104164. [CrossRef]
84. Montcho, M.; Padonou, E.A.; Montcho, M.; Mutua, M.N.; Sinsin, B. Perception and Adaptation Strategies of Dairy Farmers towards Climate Variability and Change in West Africa. *Clim. Chang.* **2022**, *170*, 38. [CrossRef]
85. Seidou, A.A.; Offoumon, O.T.L.F.; Worogo, S.H.S.; Houaga, I.; Yarou, A.K.; Azalou, M.; Boukari, F.Z.A.; Idrissou, Y.; Houinato, M.; Traoré, I.A. The Effect of the Silvopastoral System on Milk Production and Reproductive Performance of Dairy Cows and Its Contribution to Adaptation to a Changing Climate in the Drylands of Benin (West-Africa). *Front. Sustain. Food Syst.* **2023**, *7*, 1236581. [CrossRef]
86. Oleggini, G.H.; Ely, L.O.; Smith, J.W. Effect of Region and Herd Size on Dairy Herd Performance Parameters. *J. Dairy Sci.* **2001**, *84*, 1044–1050. [CrossRef]
87. Silva, C.M.; Costa Júnior, C.E.O. 228Ra in Cow's Milk from an Anomalous Region of Pernambuco-Brazil. *Int. J. Environ. Stud.* **2019**, *76*, 357–369. [CrossRef]
88. Oumou, S.H.; Samuel, N.B.; Salif, K.; Valérie, B.M.C. Analysis of Dairy Farming Systems in the Sahelian Zone of Burkina Faso. *Trop. Anim. Health Prod.* **2022**, *54*, 92. [CrossRef] [PubMed]
89. Wankar, A.K.; Rindhe, S.N.; Doijad, N.S. Heat Stress in Dairy Animals and Current Milk Production Trends, Economics, and Future Perspectives: The Global Scenario. *Trop. Anim. Health Prod.* **2021**, *53*, 70. [CrossRef]
90. Brizga, J.; Kurppa, S.; Heusala, H. Environmental Impacts of Milking Cows in Latvia. *Sustainability* **2021**, *13*, 784. [CrossRef]
91. Froldi, F.; Lamastra, L.; Trevisan, M.; Mambretti, D.; Moschini, M. Environmental Impacts of Cow's Milk in Northern Italy: Effects of Farming Performance. *J. Clean. Prod.* **2022**, *363*, 132600. [CrossRef]
92. Darré, E.; Llanos, E.; Astigarraga, L.; Cadenazzi, M.; Picasso, V. Do Pasture-Based Mixed Dairy Systems with Higher Milk Production Have Lower Environmental Impacts? A Uruguayan Case Study. *New Zealand J. Agric. Res.* **2021**, *64*, 444–462. [CrossRef]
93. Wilkinson, J.M.; Chamberlain, A.T.; Rivero, M.J. The Case for Grazing Dairy Cows. *Agronomy* **2021**, *11*, 2466. [CrossRef]
94. Castro, C.N. *Aspectos Socieconômicos da Região do Matopiba*; Instituto de Pesquisa Econômica Aplicada (IPEA): Brasília, Brazil, 2018.
95. Godde, C.M.; Boone, R.B.; Ash, A.J.; Waha, K.; Sloat, L.L.; Thornton, P.K.; Herrero, M. Global Rangeland Production Systems and Livelihoods at Threat under Climate Change and Variability. *Environ. Res. Lett.* **2020**, *15*, 044021. [CrossRef]
96. Wróbel, B.; Zielewicz, W.; Staniak, M. Challenges of Pasture Feeding Systems—Opportunities and Constraints. *Agriculture* **2023**, *13*, 974. [CrossRef]
97. Hu, W.; Drewry, J.; Beare, M.; Eger, A.; Müller, K. Compaction Induced Soil Structural Degradation Affects Productivity and Environmental Outcomes: A Review and New Zealand Case Study. *Geoderma* **2021**, *395*, 115035. [CrossRef]
98. FAO. *The State of Food and Agriculture*, 1st ed.; FAO: Rome, Italy, 2009; Volume 1.
99. Gosch, M.S.; Parente, L.L.; Santos, C.O.; Mesquita, V.V.; Ferreira, L.G. Landsat-Based Assessment of the Quantitative and Qualitative Dynamics of the Pasture Areas in Rural Settlements in the Cerrado Biome, Brazil. *Appl. Geogr.* **2021**, *136*, 102585. [CrossRef]
100. Duguma, B. Farmers' Perceptions of Major Challenges to Smallholder Dairy Farming in Selected Towns of Jimma Zone, Oromia Regional State, Ethiopia: Possible Influences, Impacts, Coping Strategies and Support Required. *Heliyon* **2022**, *8*, e09581. [CrossRef]

101. Salvati, L.; Mavrakis, A.; Colantoni, A.; Mancino, G.; Ferrara, A. Complex Adaptive Systems, Soil Degradation and Land Sensitivity to Desertification: A Multivariate Assessment of Italian Agro-Forest Landscape. *Sci. Total Environ.* **2015**, *521–522*, 235–245. [CrossRef] [PubMed]
102. Zeraatpisheh, M.; Ayoubi, S.; Sulieman, M.; Rodrigo-Comino, J. Determining the Spatial Distribution of Soil Properties Using the Environmental Covariates and Multivariate Statistical Analysis: A Case Study in Semi-Arid Regions of Iran. *J. Arid. Land* **2019**, *11*, 551–566. [CrossRef]
103. Silva, M.V.; Pandorfi, H.; Lopes, P.M.O.; Silva, J.L.B.; Almeida, G.L.P.; Silva, D.A.O.; Santos, A.; Rodrigues, J.A.M.; Batista, P.H.D.; Jardim, A.M.R.F. Pilot Monitoring of Caatinga Spatial-Temporal Dynamics through the Action of Agriculture and Livestock in the Brazilian Semiarid. *Remote Sens. Appl.* **2020**, *19*, 100353. [CrossRef]